Solid Flame:
Fundamentals and Applications

Combustion: Definitions

- an act or instance of burning
- a usually rapid **chemical process** (as ***oxidation***) that produces **heat** and usually light;
- *also* **:** a slower oxidation (as in the body)
- a chemical process in which a substance *reacts* **vigorously** with ***oxygen*** to produce heat and light, seen as a flame
- the burning of fuel in an engine to provide power

Combustion or **burning** is a complex sequence of exothermic chemical reactions between a fuel and an oxidant accompanied by the production of heat or both heat and light in the form of either a glow or flames.
A simpler example can be seen in the combustion of hydrogen and oxygen, which is a commonly used reaction in rocket engines:

$$2H_2 + O_2 \rightarrow 2H_2O + \text{heat}$$

The result is simply water vapor.

The Phenomenon of Wave Localization for Solid State Self-propagating Reactions:

SOLID FLAME

A.G. Merzhanov, V.M. Shkiro, I.P. Borovinskaya, 1967

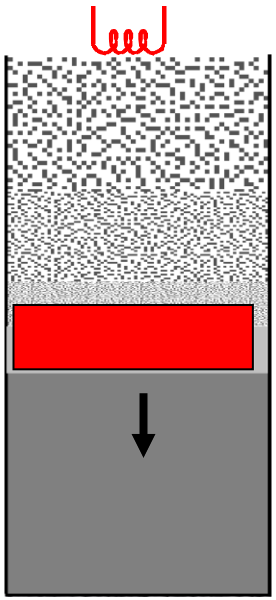

Combustion products (solid)

Combustion zone (solid)

Initial reagents (solid)

$$Ta + C \rightarrow ½\ Ta_2C + ½\ C + Q_1 \rightarrow TaC + Q_2$$

$$T_{ad} = 2730\ K,\ T_m = 3100\ K$$

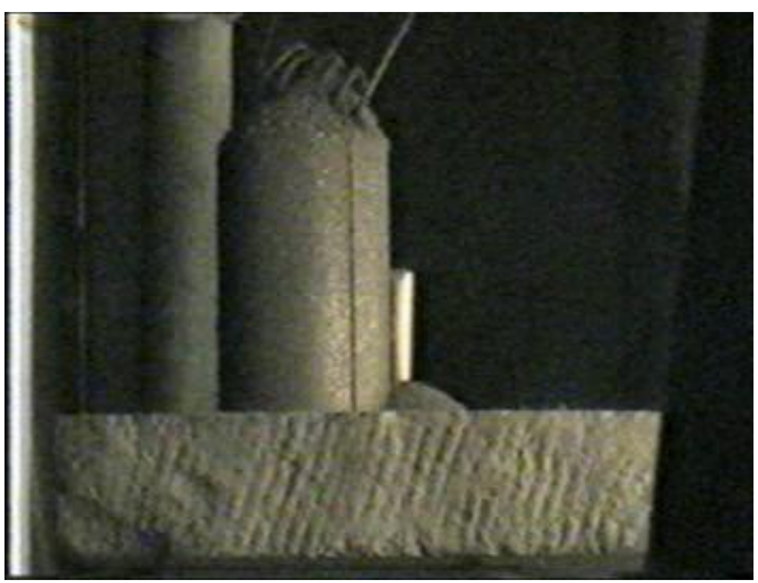

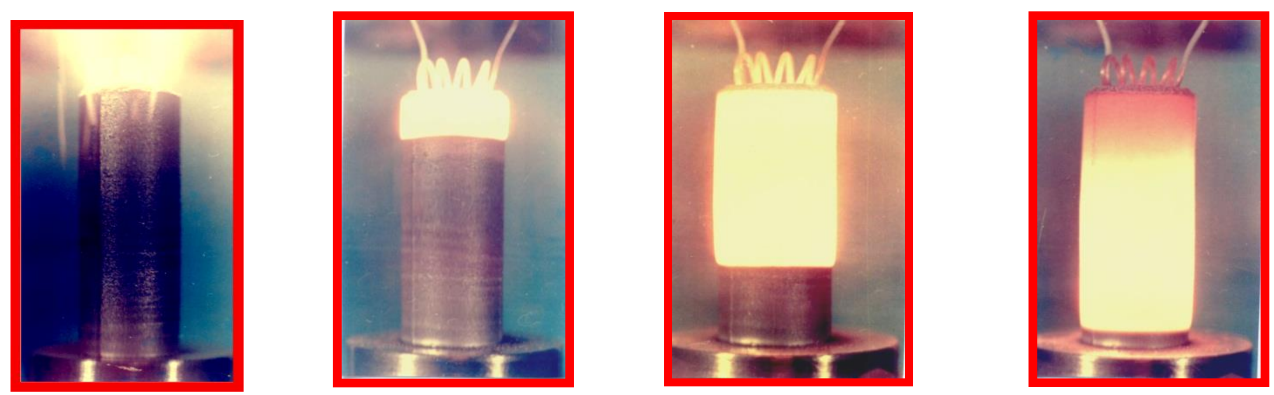

ignition

front propagation

cooling

Tantalum - Graphite *System*

Physical Properties	**Tantalum**
Atomic Number	180.95
Density	16.6 g/cc
Melting Point	**3290 K, 2996°C**
Boiling Point	**5731 K, 6100°C**
Thermal Conductivity (20°C)	57.8 $Wm^{-1}K^{-1}$
Thermal diffusivity	0.2 cm^2/s
Heat of fusion	37 $kJmol^{-1}$
Heat of vaporization	733 $kJmol^{-1}$

Physical Properties	**Graphite**
Atomic Number	12.0
Density	2.27 g/cc
Melting Point	**4300 K, 4027°C**
Boiling Point	**4000 K, 3727°C**
Thermal Conductivity (20°C)	1-2 10^3 $Wm^{-1}K^{-1}$
Thermal diffusivity	0.5-1.3 cm^2/s
Heat of fusion	100 $kJmol^{-1}$
Heat of vaporization	355$kLmol^{-1}$

2-5 μm

0.1-1 μm

Thermodynamic Considerations

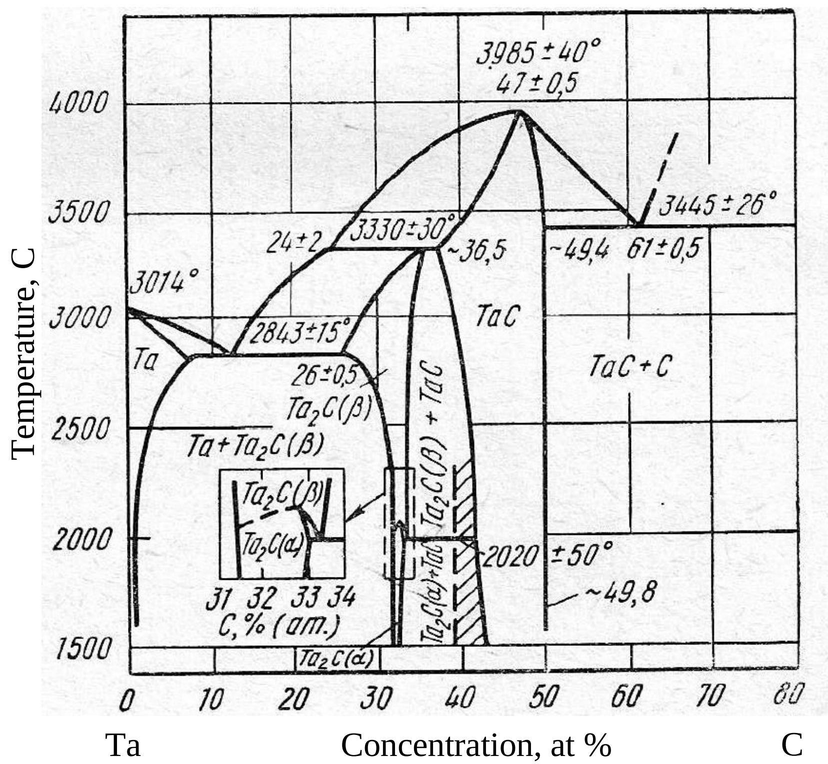

Volume of gas products	(liters)	**0.0000**
Pressure of gas products	(atm)	1.0000
Temperature	(K)	**2744**
Gas products amount	(mol)	6.00E-15
Products heat capacity	(J/K)	74.30
Products entropy	(J/K)	161.2
Products enthalpy	(KJ)	0.677
Ta1C 1	**(S)**	**1.0000**

Ta + C = TaC + Q

Q=144 kJ/mol

Tantalum carbide (TaC) is an extremely hard refractory (3880°C; 4153 K) ceramic material, commercially used in tool bits for cutting tools.
It is a heavy, brown powder usually processed by sintering.
Tantalum carbide-graphite composite material, developed in Los Alamos National Laboratory, is one of the hardest materials ever synthesized.

"Solid Flame":

Ta + C - Recent Advances (2011)

Nano-Structure of Composite Ta-C particle

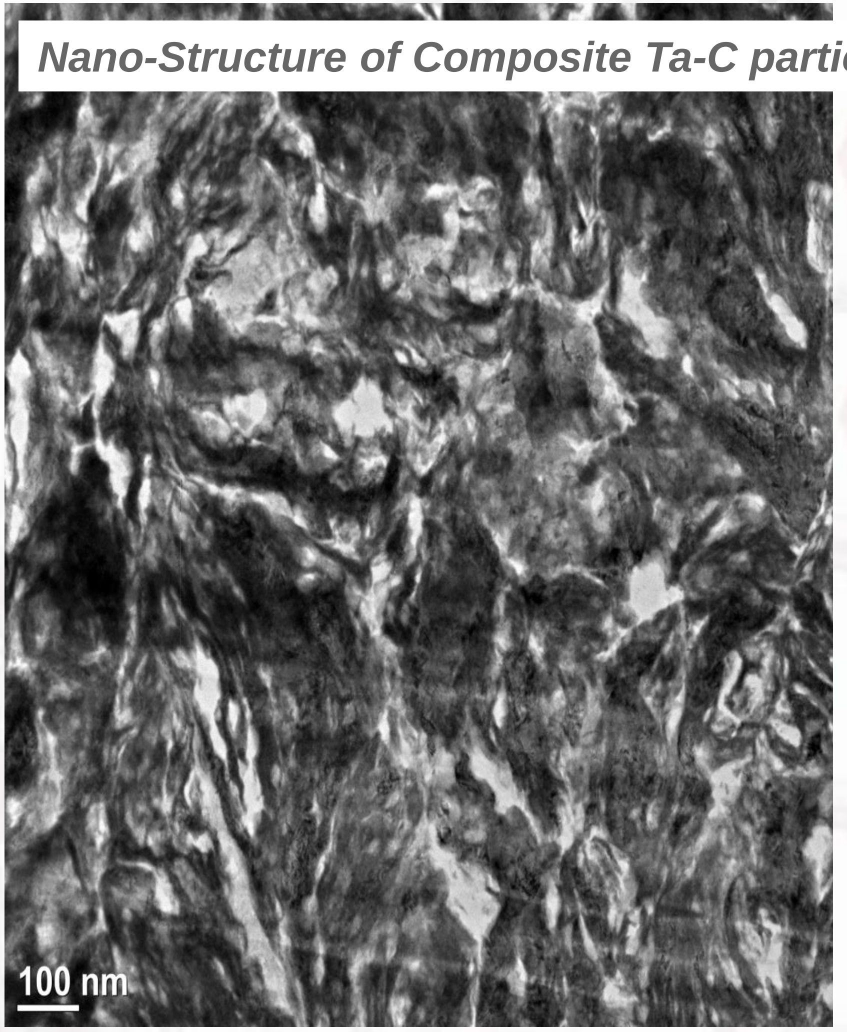

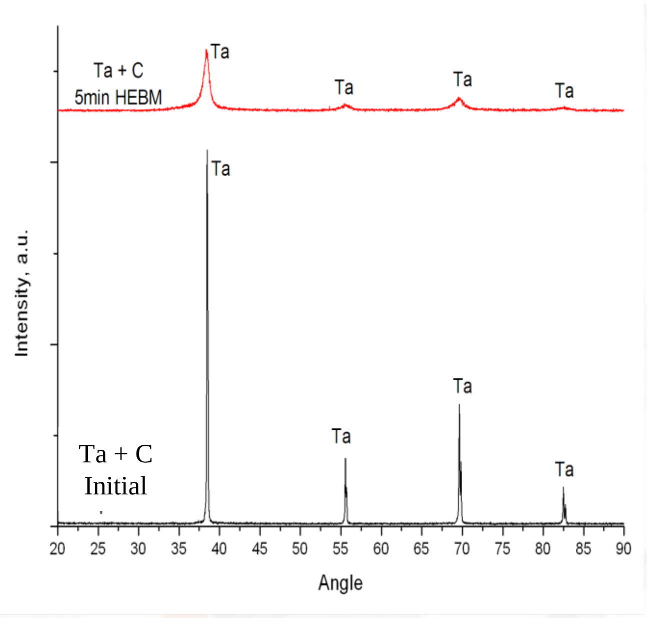

Comparison of XRD patterns for Ta-C system before (a) and after (b) HEBM

Reaction Front Propagation in Ta-C Heterogeneous System

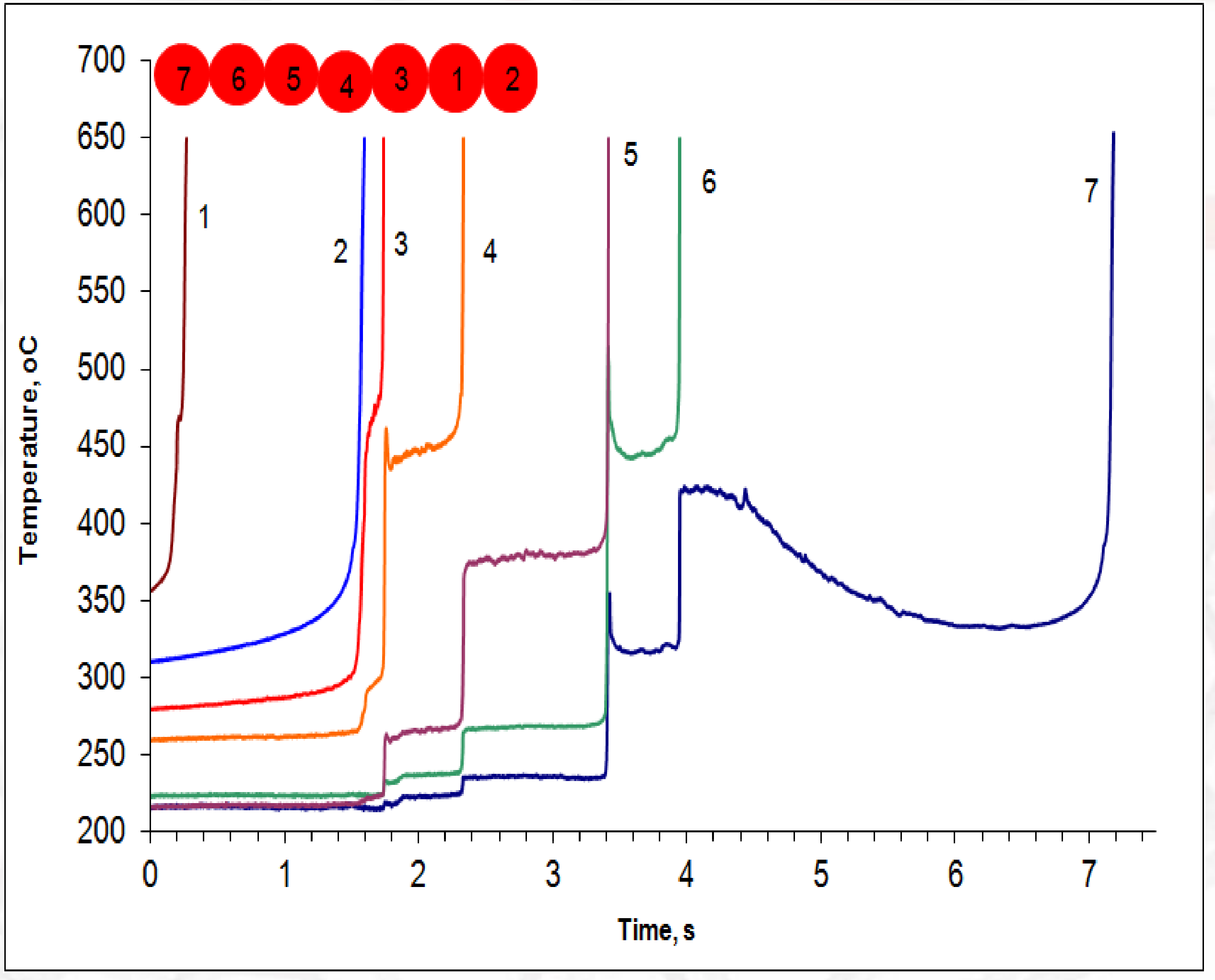

TECHNOLOGY FOR MATERIAL SYNTHESIS:

Self-propagating High-temperature Synthesis (SHS)

Or Combustion Synthesis

Gasless Combustion Systems

$$\sum_{i=1}^{n} X_i^{(s)} = \sum_{j=1}^{m} P_j^{(s,l)} + Q,$$

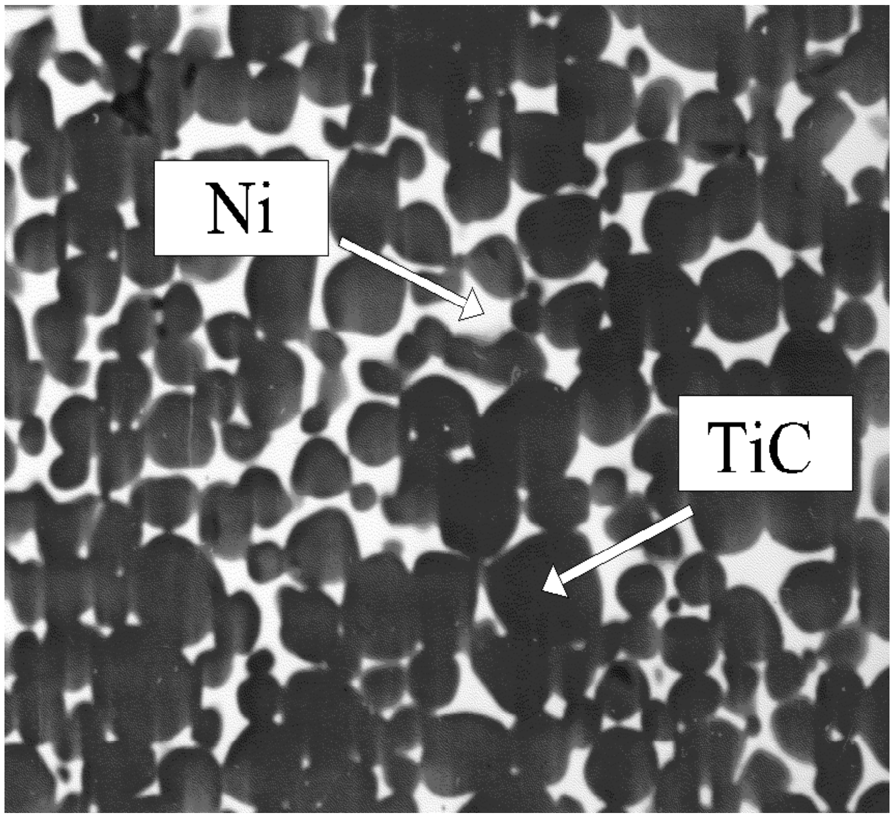

Ti + C + Ni = TiC + Ni
+ 230 kJ/mol.

System	Adiabatic Comb. Temp. T_c^{ad}, K	Measured Comb. Temp. T_c, K	Lowest Melting Point Phase Diagram, K
<u>Carbides</u>	3290	2550	3295 (Ta)
Ta + C	1690	3070	1921 (eut)
Ti + C	1690	3000	1690 (Si)
Si + C			
<u>Borides</u>			
Ta + B	2728	2700	2365 (B)
Ti+2B	3193	3190	1810 (eut)
Ti + B	2460	2500	1810 (eut)
<u>Silicides</u>			
Mo + 2Si	1925	1920	1673 (eut)
Ti + 2Si	1773	1770	1600 (eut)
5Ti + 3Si	2403	2350	1600 (eut)
<u>Intermetallics</u>			
Ni + Al	1912	1900	921 (eut)
3Ni + Al	1586	1600	921 (eut)
Ti + Al	1517	n/a	933 (Al)
Ti + Ni	1418	n/a	1215 (eut)
Ti + Fe	1042	n/a	1358 (eut)

Gas-Solid Combustion Systems

$$\sum_{i=1}^{n-p} X_i^{(s)} + \sum_{i=1}^{p} Y_i^{(g)} = \sum_{j=1}^{m} P_j^{(s,l)} + Q,$$

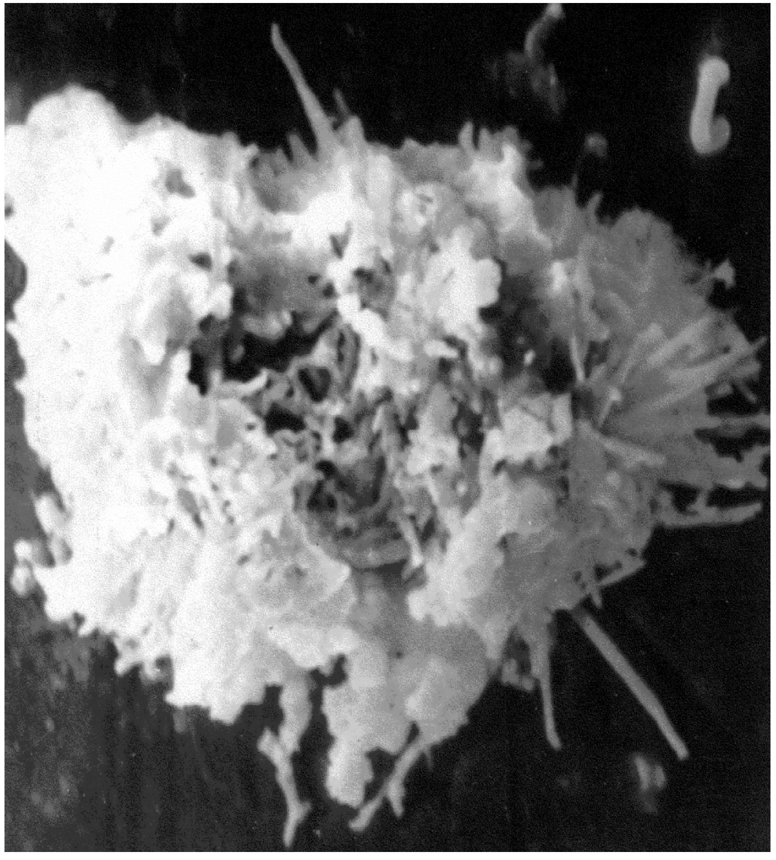

System	Adiabatic Comb. Temp. T_c^{ad}, K	Measured Comb. Temp. T_c, K	Lowest Melting Point Phase Diagram, K
Nitrides†			
2Ta + N2	3165	2500	3000 (Ta)
2Nb + N2	3322	2800	2673 (NbN)
2Ti + N2	3446	2700	1943 (Ti)
2Al + N2	3639	2300	933 (Al)
3Si + 2N2	2430	2250	1690 (Si)
2B + N2	3437	2600	2350 (B)

$Ti(s) + 0.5N_2(g) = TiN(s) + 335$ kJ/mol,
$3Si(s) + 2N_2(g) = Si_3N_4(s) + 750$ kJ/mol.

Reduction Combustion Systems

$$\sum_{i=1}^{n-q-r}(MO_x)_i^{(s)}+\sum_{i=1}^{r}Z_i^{(s)}+\sum_{i=1}^{q}X_i^{(s)}=\sum_{j=1}^{m-k}P_j^{(s,l)}+\sum_{j=1}^{k}(ZO_y)_j^{(s,l)}+Q,$$

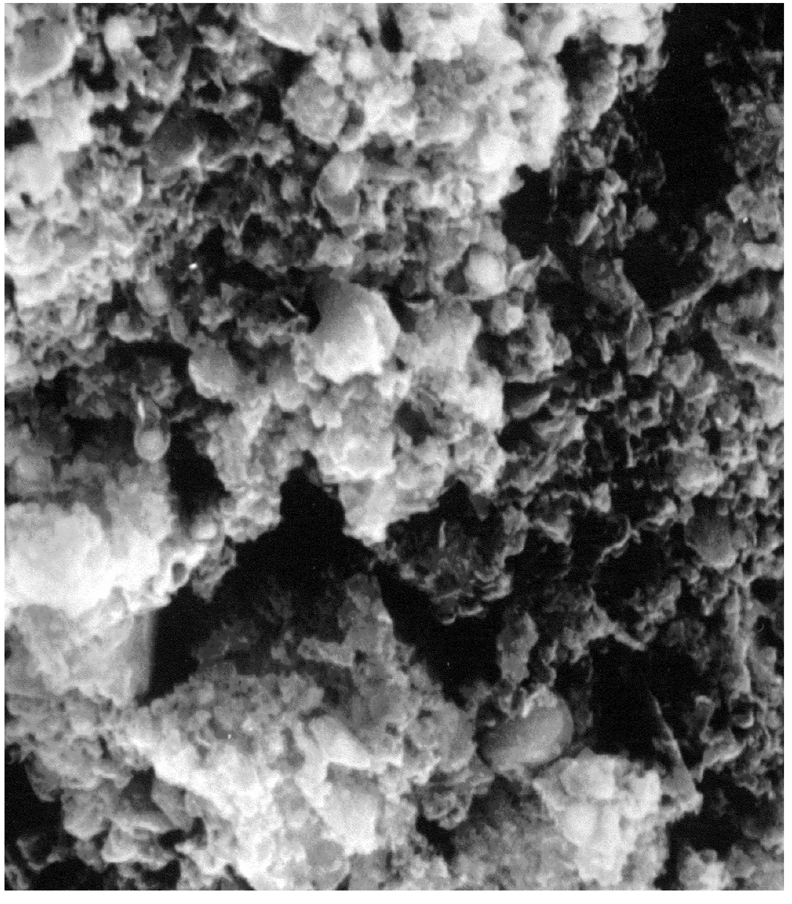

System	Adiabatic Comb. Temp. T_c^{ad}, K	Measured Comb. Temp. T_c, K	Lowest Melting Point Phase Diagram, K
B_2O_3 + Mg	2530	2420	1415 (eut)
B_2O_3 + Mg + C	2400	2270	n/a
B_2O_3 + Mg + N_2	2830	2700	n/a
SiO_2 + Mg	2250	2200	1816 (eut)
SiO_2 + Mg + C	2400	2330	n/a
La_2O_3 + Mg + B_2O_3	n/a	2400	n/a

$$B_2O_3(s) + 2Al(s) + Ti(s) = Al_2O_3(l) + TiB_2(s,l) + 700\ kJ/mol,$$

Diamond - Intermetallics Composites

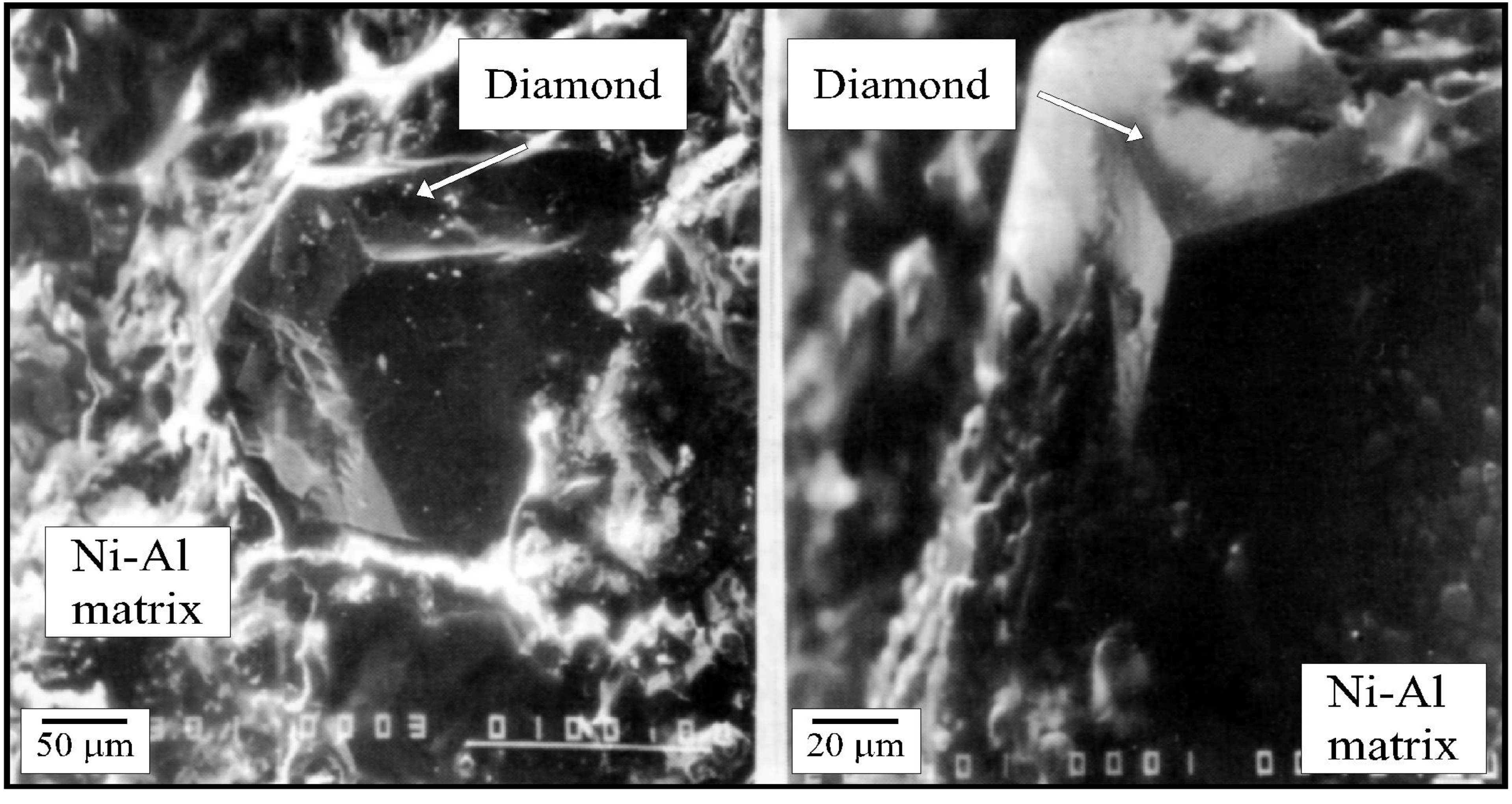

Gasless Combustion to Produce Advanced Materials

CS-PRODUCTS: Cermets

Self-Sustained Gasless Heterogeneous Reactions:

Fundamentals

Characteristic Structure of Combustion Wave

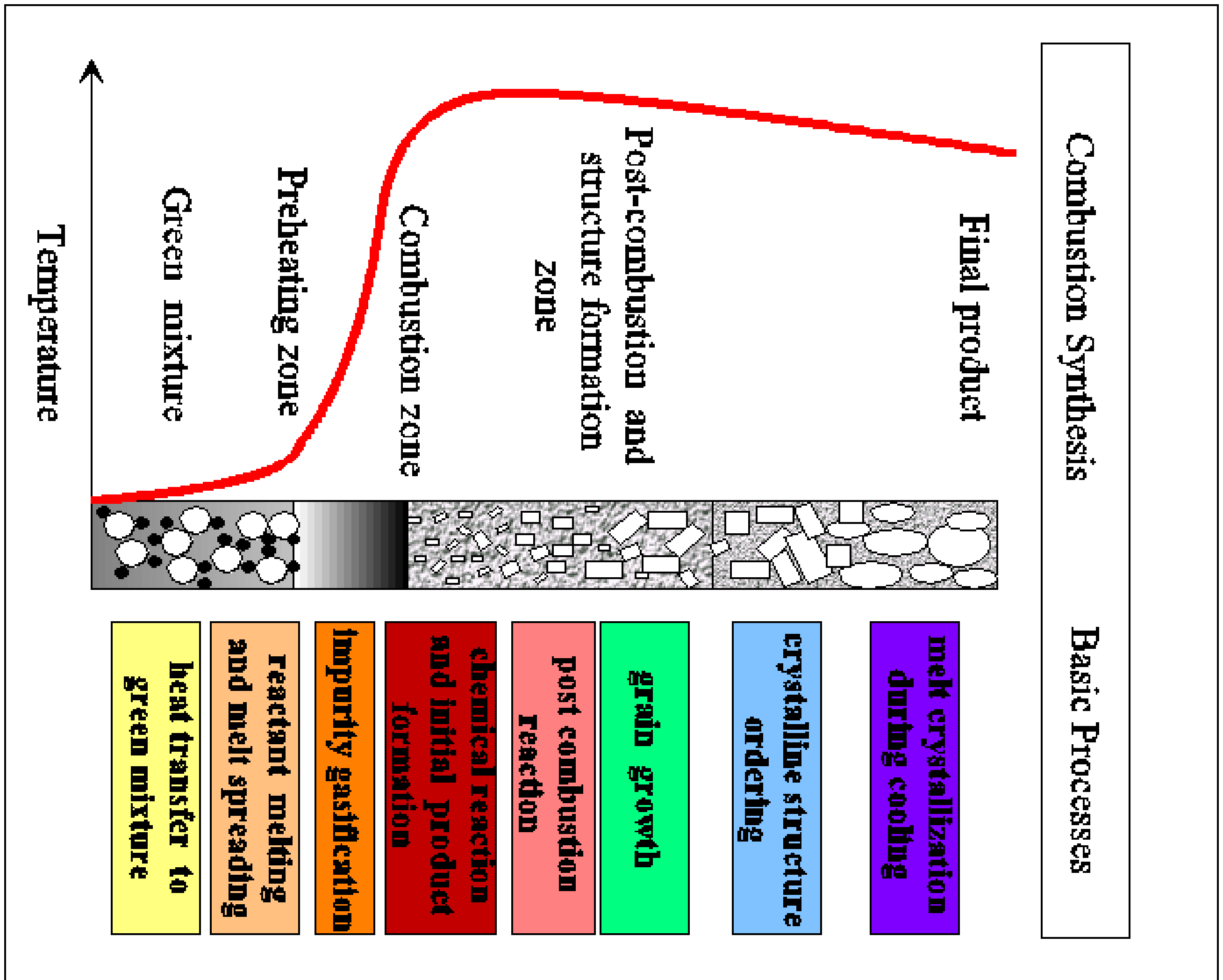

Dynamic Methods
for Rapid Heterogeneous
High-Temperature Reactions

Quasi-homogeneous Model

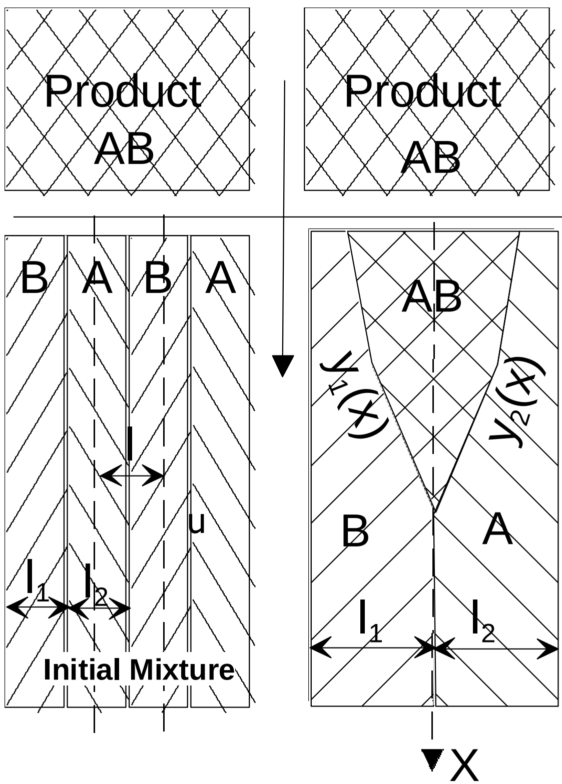

$$-u\cdot\frac{\partial c}{\partial x}=\frac{\partial}{\partial x}\cdot(D\cdot\frac{\partial c}{\partial x})+\frac{\partial}{\partial y}\cdot(D\cdot\frac{\partial c}{\partial y})\qquad y_1(x)<y<y_2(x)$$

$$-u\cdot\frac{\partial T}{\partial x}=\frac{\partial}{\partial x}\cdot(a\cdot\frac{\partial T}{\partial x})+\frac{\partial}{\partial y}\cdot(a\cdot\frac{\partial T}{\partial y})\qquad -l_1<y<l_2$$

$$y=y_1\quad -l_1<y_1<0:\quad c=c_1,\quad D\left(\frac{\partial c}{\partial y}-\frac{\partial c}{\partial x}\frac{\partial y_1}{\partial x}\right)=uc_1\cdot\frac{\partial y_1}{\partial x}$$

$$a\left(\frac{\partial T}{\partial x}\cdot\frac{\partial y_1}{\partial x}-\frac{\partial T}{\partial y}\right)=\frac{Q}{c_s}u\cdot\frac{\partial y_1}{\partial x}$$

$$y=y_2\quad 0<y_1<l_2:\quad c=c_2,\quad D\left(\frac{\partial c}{\partial y}-\frac{\partial c}{\partial x}\frac{\partial y_2}{\partial x}\right)=-u(1-c_2)\cdot\frac{\partial y_2}{\partial x}$$

$$a\left(\frac{\partial T}{\partial x}\cdot\frac{\partial y_2}{\partial x}-\frac{\partial T}{\partial y}\right)=\frac{Q}{c_s}u\cdot\frac{\partial y_2}{\partial x}$$

$$x\to+\infty:\quad T=T_0,\ y_1=y_2=0$$

$$x\to-\infty:\quad y_1=-l_1;\ y_1=l_2,\quad \frac{\partial c}{\partial x}=\frac{\partial c}{\partial y}=0,\quad \frac{\partial T}{\partial x}=\frac{\partial T}{\partial y}=0$$

$$\varepsilon=\frac{D}{\alpha}<<1$$

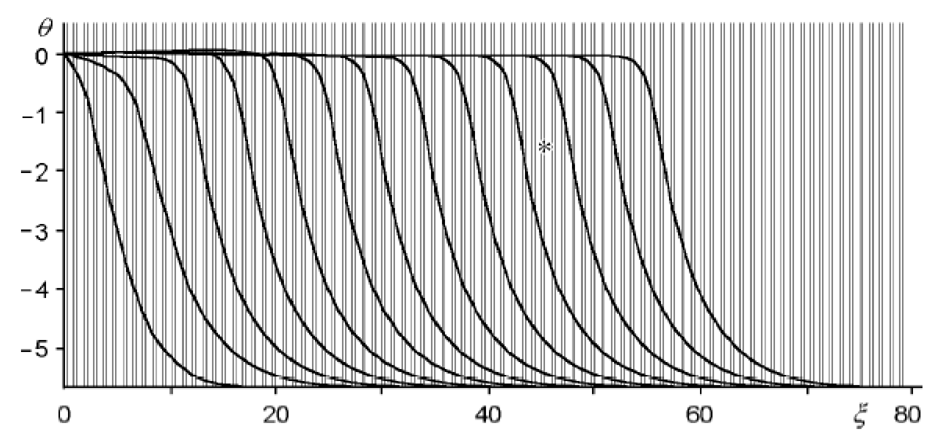

Aldushin A.P., Martem’yanova T.M., **Merzhanov A.G.**, Khaikin B.I., Shkadinskii K.G. Combustion Explosion Shock Wave, *1972, 8(2), 202*

Characteristic Temperature Profiles

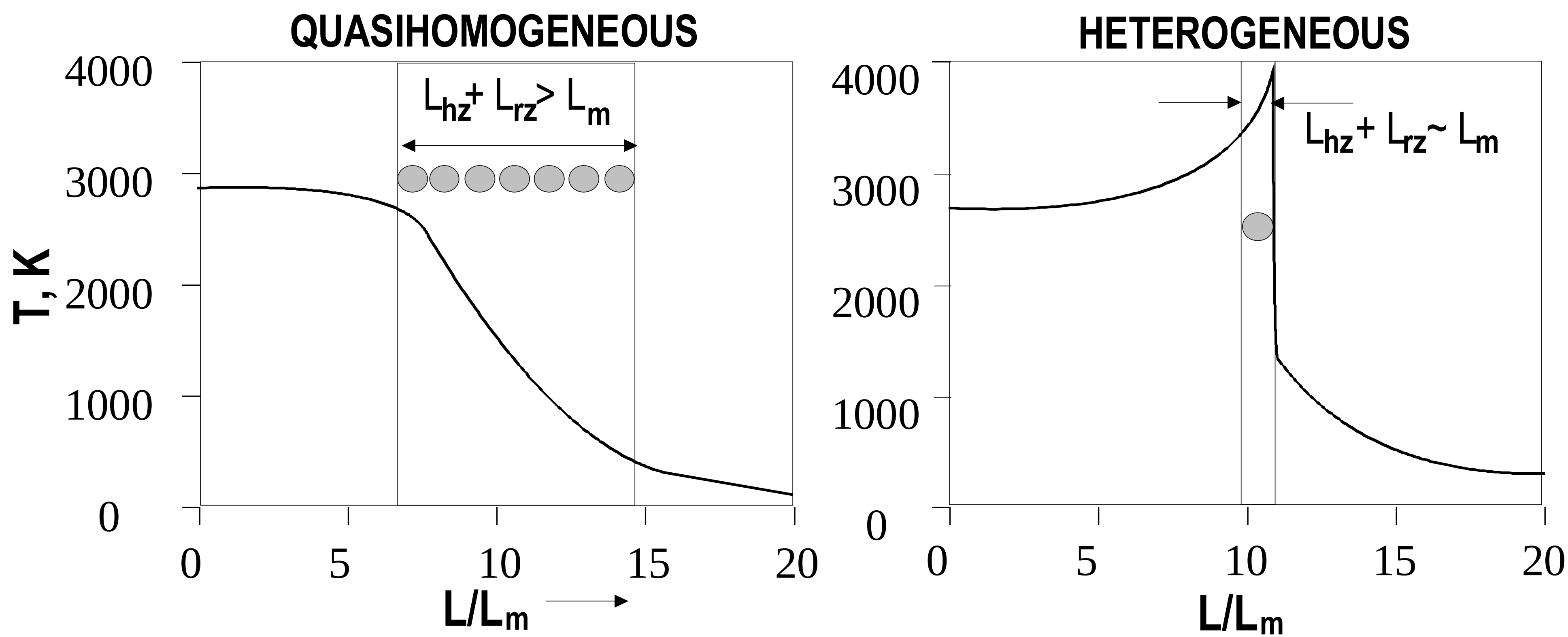

High-Speed Micro Video Recording

Digital High-Speed Microscopic Video Recording Technique

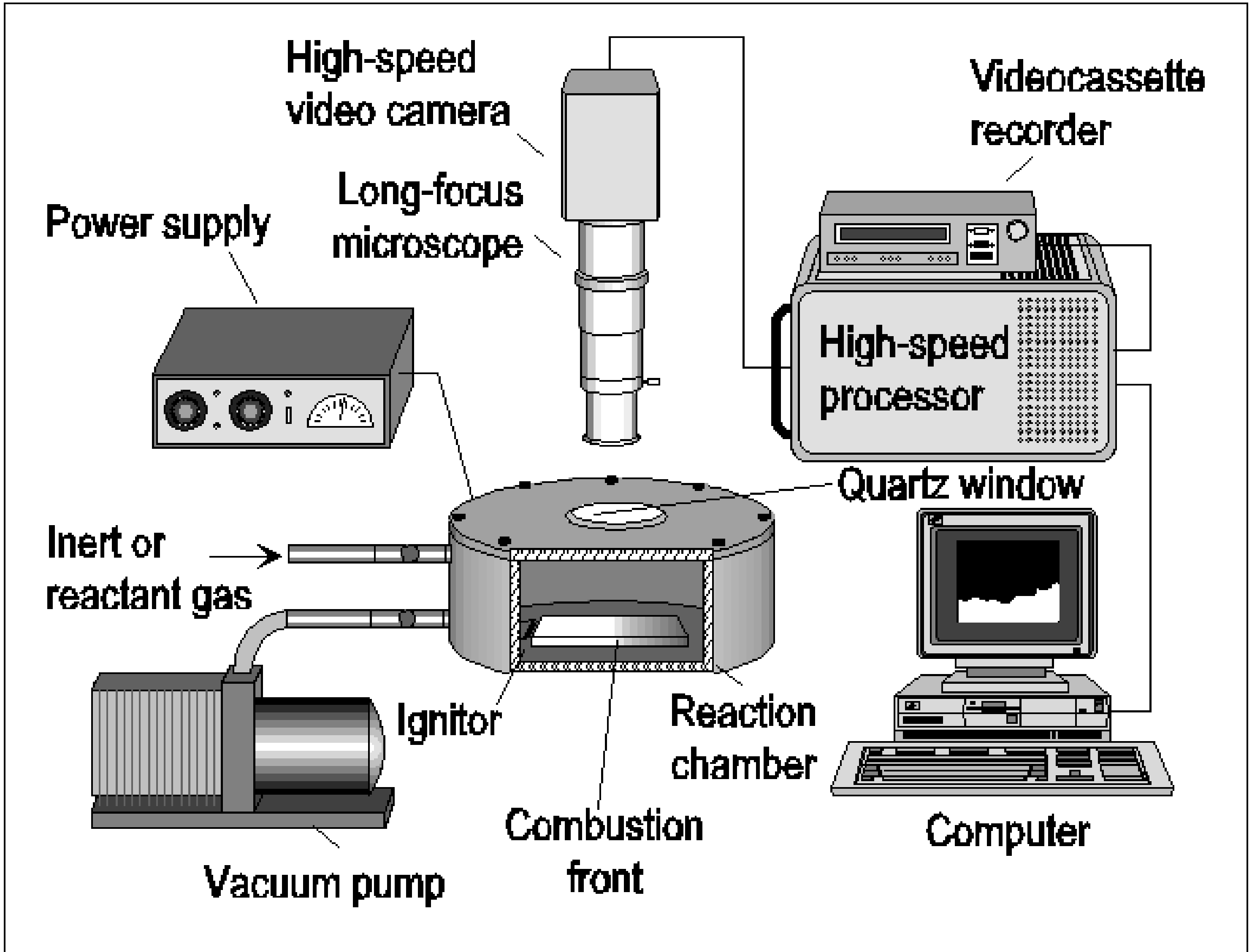

Recording rate:

up to 12,000 fr./s

Magnification:

up to 800x

Instantaneous Velocity

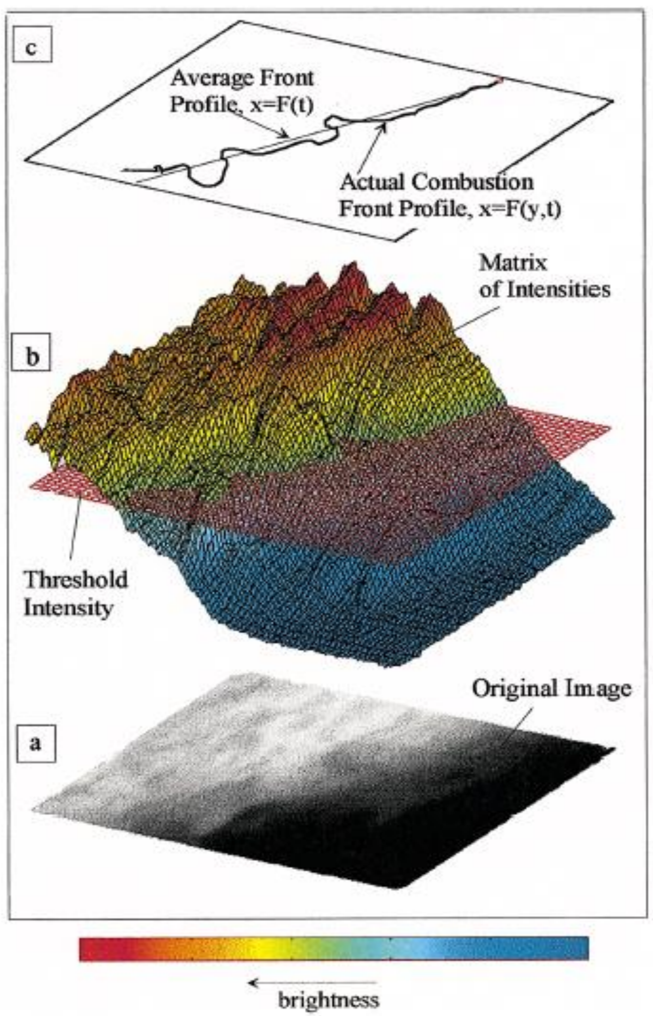

$$U(y,t) = \frac{\partial F(y,t)}{\partial t} \approx \frac{F(y,t_j) - F(y,t_{j-1})}{t_j - t_{j-1}}.$$

$$\bar{U} = \frac{\int_{t_i}^{t_f} \int_0^{y_0} U(y,t)\,\mathrm{d}y\,\mathrm{d}t}{y_0(t_f - t_0)},$$

$$\sigma_U = \sqrt{\frac{\int_{t_i}^{t_f} \int_0^{y_0} [\bar{U} - U(y,t)]^2\,\mathrm{d}y\,\mathrm{d}t}{y_0(t_f - t_i)}}.$$

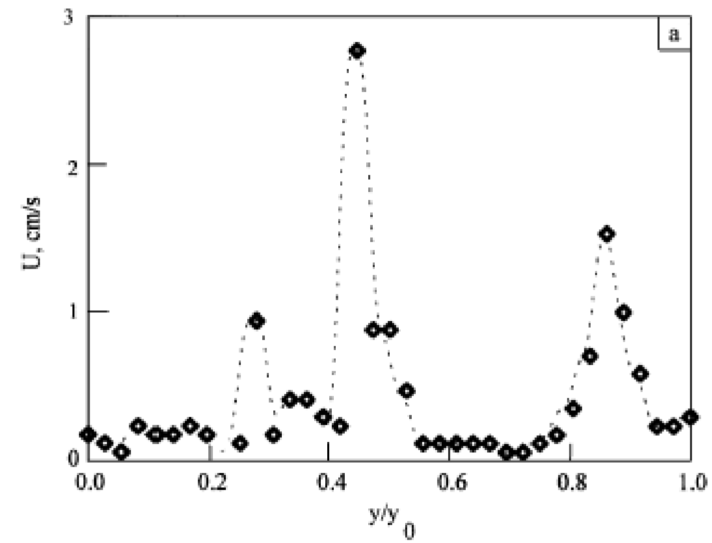

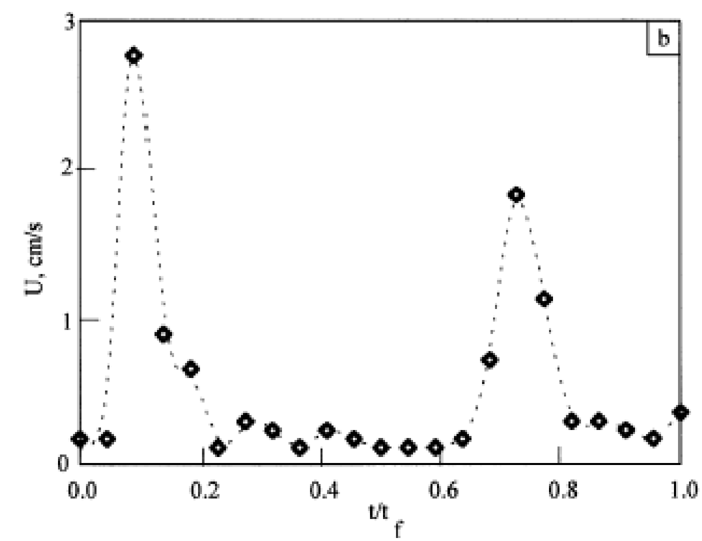

Distribution of Instantaneous Combustion Velocity

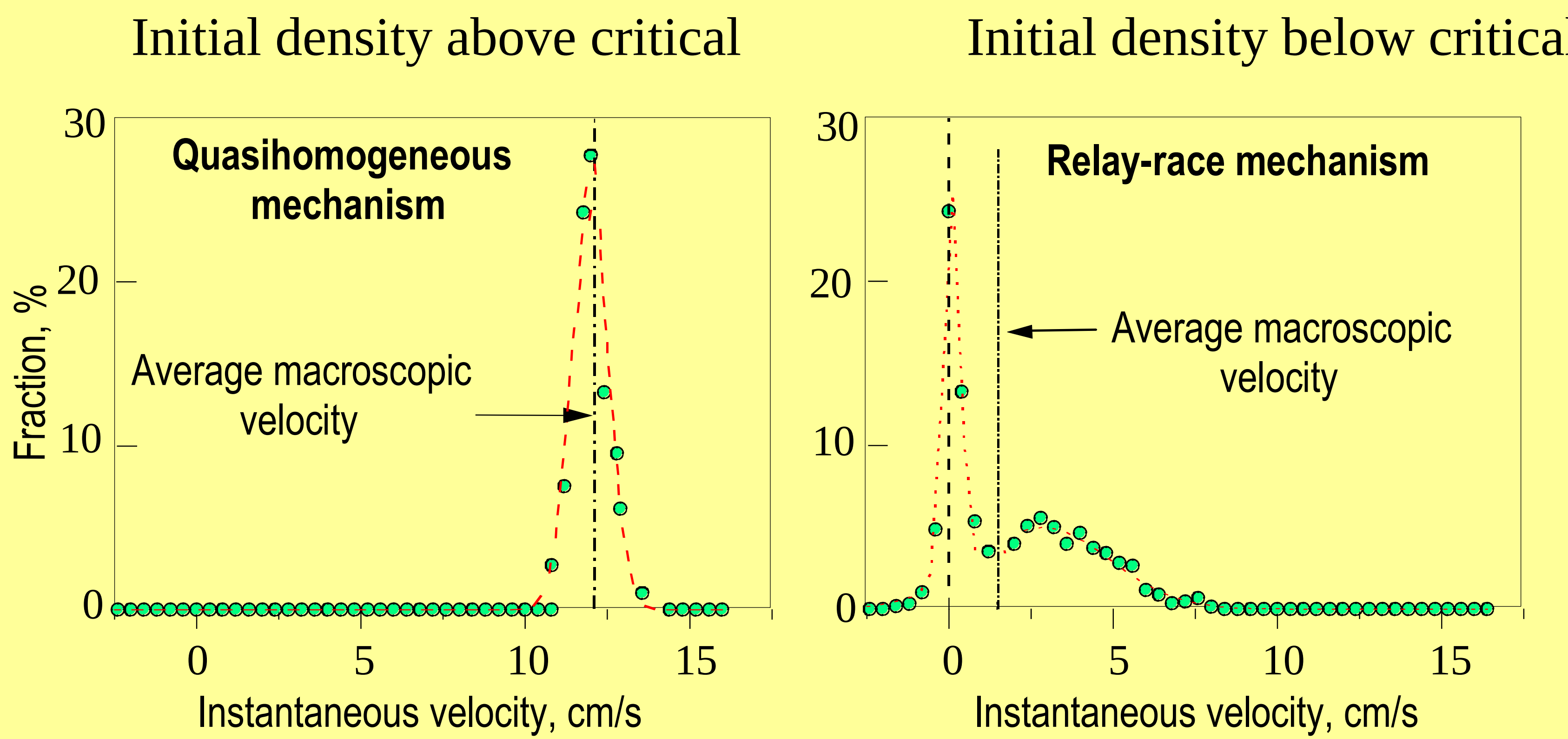

Thermal Structures of Heterogeneous Reaction Wave

Super-adiabatic peaks

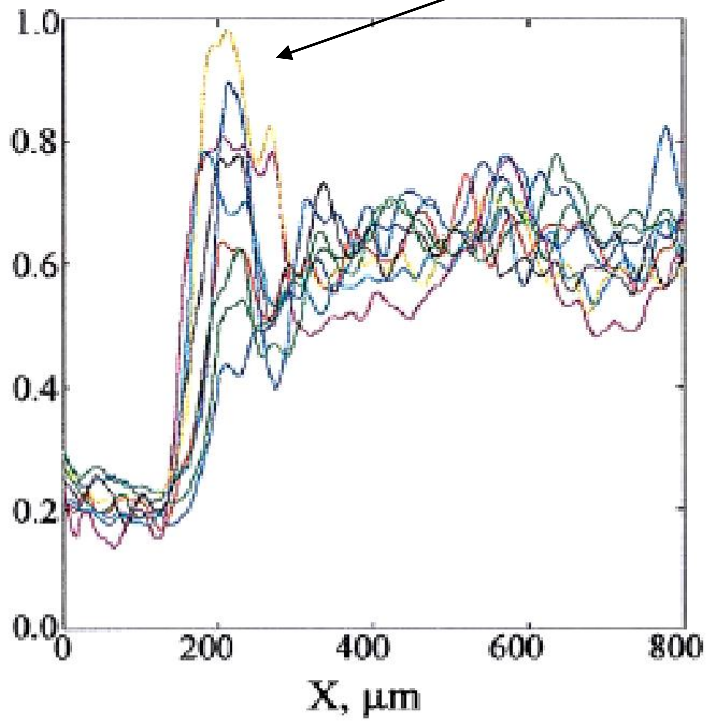

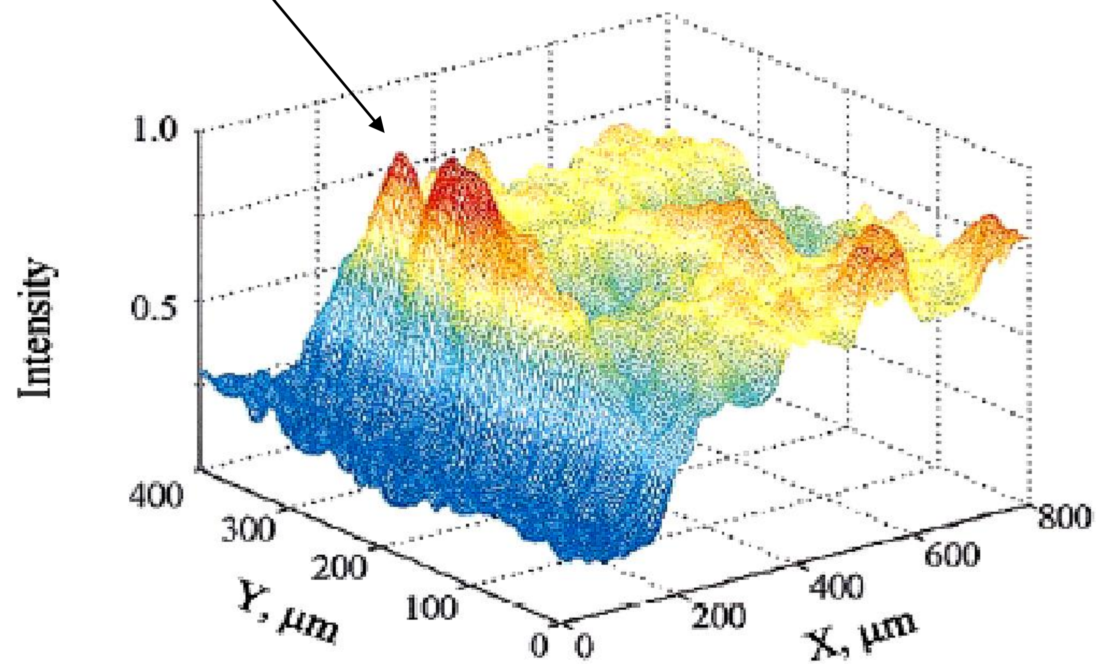

Structure of Reaction Front

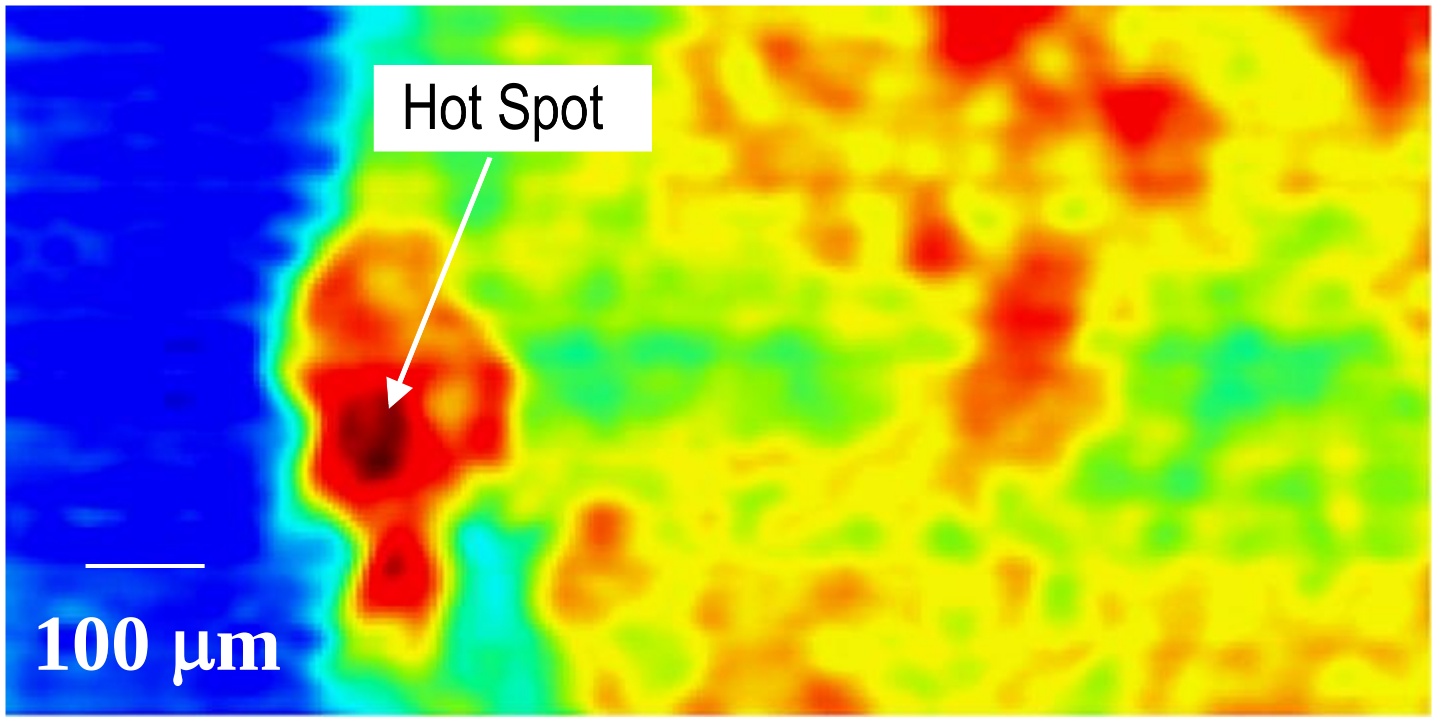

Direction of Combustion Front Propagation

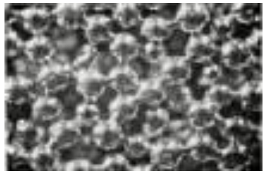

Thermal Conductivity of the Heterogeneous Media

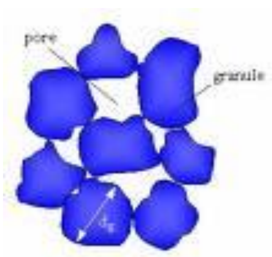

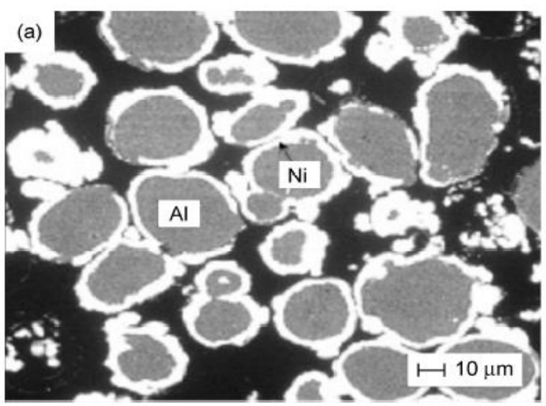

$$m_A = \frac{\int_0^{x_0} m_A(x)dx}{x_0}$$

$$\sigma_A = \frac{\int_0^{x_0} \sigma_A(x)dx}{x_0}$$

$$m_A(x) = \tan(\Theta)$$

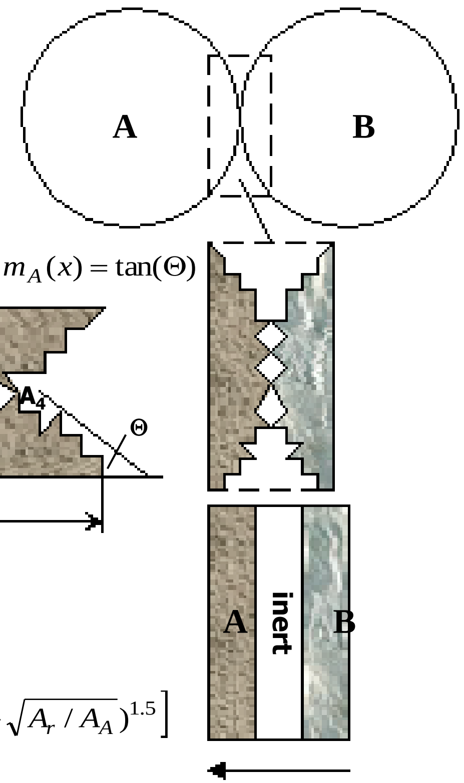

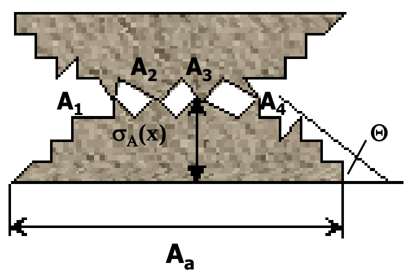

$$A_r = \sum_i A_i$$

$$k_c = \left[2k_s\sigma_A n/(1-\sqrt{A_r/A_A})^{1.5}\right]$$

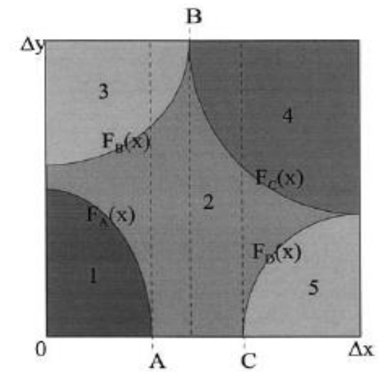

Electrical analogy

$$k_x = \int_0^A [R_1 F_A(x) + R_2(F_B(x) - F_A(x)) + R_3(\Delta y - F_B(x))]^{-1}\,\mathrm{d}x + \int_A^B [R_2 F_B(x) + R_3(\Delta y - F_B(x))]^{-1}\,\mathrm{d}x + \int_B^C [R_2 F_C(x) + R_4(\Delta y - F_C(x))]^{-1}\,\mathrm{d}x + \int_C^{\Delta x} [R_5 F_D(x) + R_2(F_C(x) - F_D(x)) + R_4(\Delta y - F_C(x))]^{-1}\,\mathrm{d}x,$$

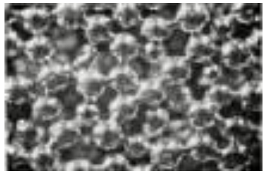

Heterogeneous Model

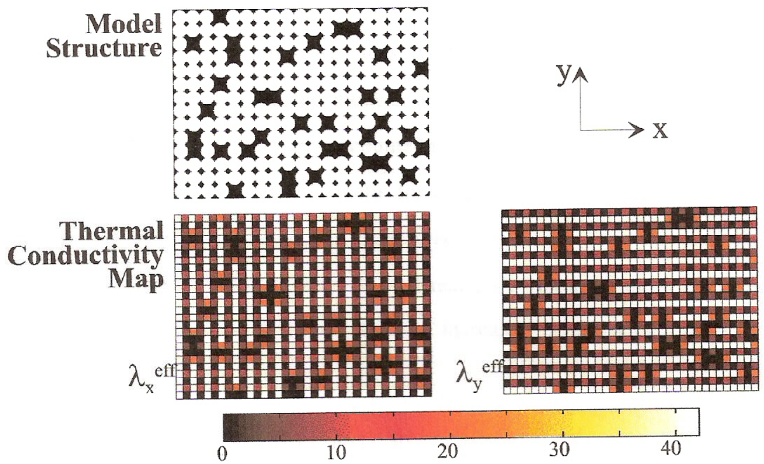

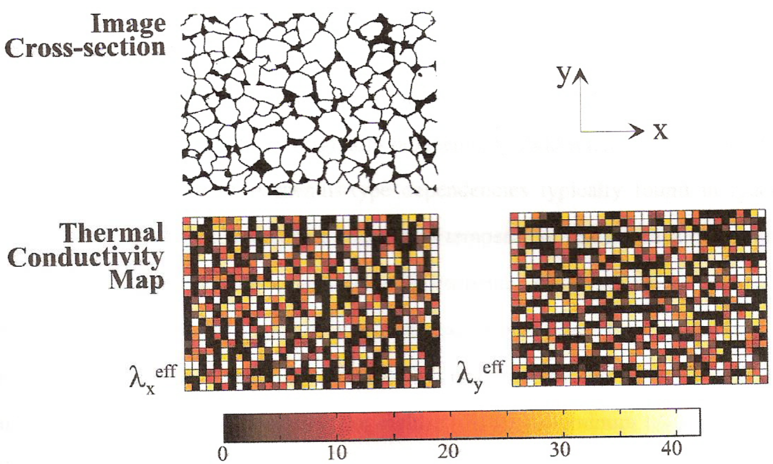

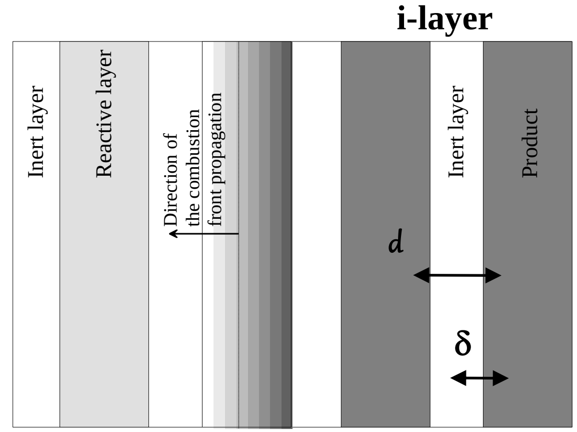

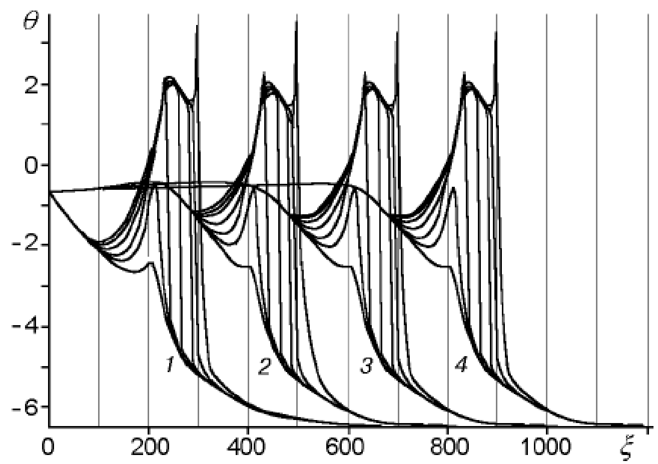

Reactive layer

$$(i-1)(d+\delta) < \xi < id + (i-1)\delta$$

$$\frac{\partial \theta}{\partial \tau} = \frac{\partial^2 \theta}{\partial \xi^2} + \frac{1}{\gamma}\frac{\partial \eta}{\partial \tau}$$

$$\frac{\partial \eta}{\partial \eta} = \gamma F(\theta, \eta)$$

Inert layer

$$id + (i-1)\delta < \xi < i(d+\delta)$$

$$\sigma_{c\rho}\frac{\partial \theta}{\partial \tau} = \sigma_{\lambda}\frac{\partial^2 \theta}{\partial \xi^2}$$

$$\sigma_{c\rho} = \frac{c_I \rho_I}{c_R \rho_R} \qquad \sigma_{\lambda} = \frac{\lambda_I}{\lambda_R}$$

$$\theta|_R = \theta|_I, \qquad \left.\frac{\partial \theta}{\partial \xi}\right|_R = \sigma_{\lambda}\left.\frac{\partial \theta}{\partial \xi}\right|_I$$

$$\tau = 0, \quad \xi > 0: \quad \theta = \theta_0, \quad \eta = 0$$

$$(T = T_0).$$

Time-Resolved X-Ray Diffraction Technique

Time-Resolved X-Ray Diffraction Technique

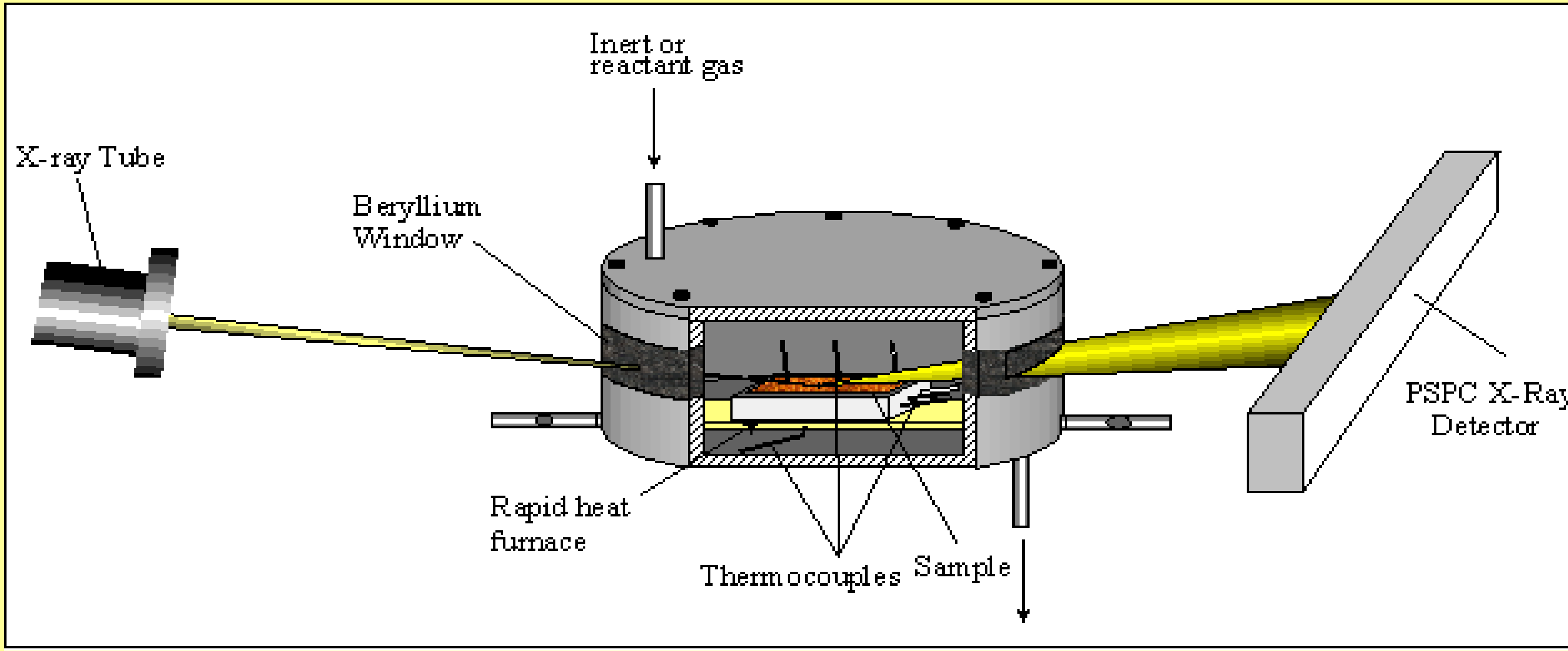

Scattering angles range: 2Θ~ 36º

Grabbing rate of diffraction patterns:up to 10^3 1/s

Titanium-Air System

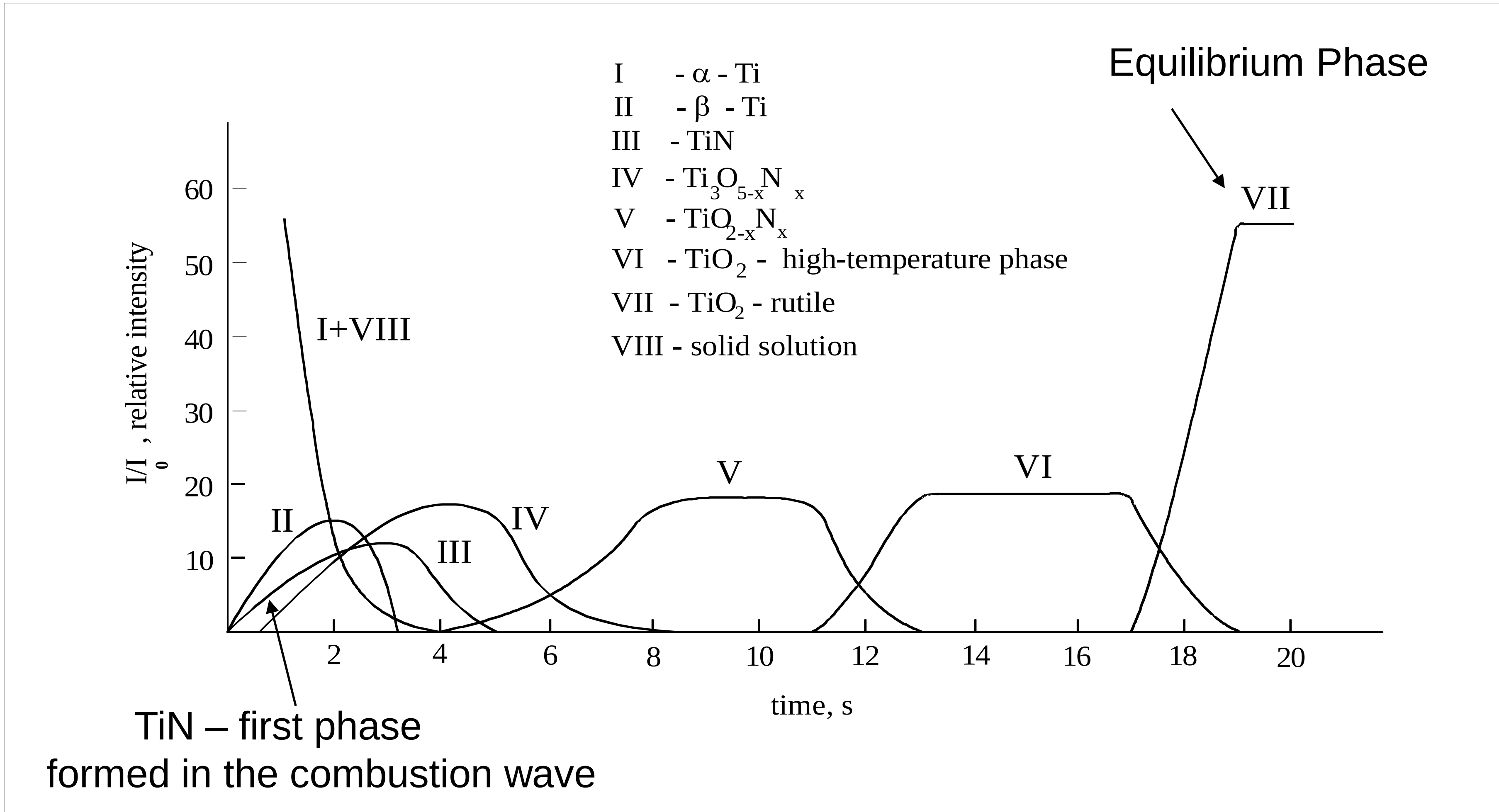

Niobium-Boron System

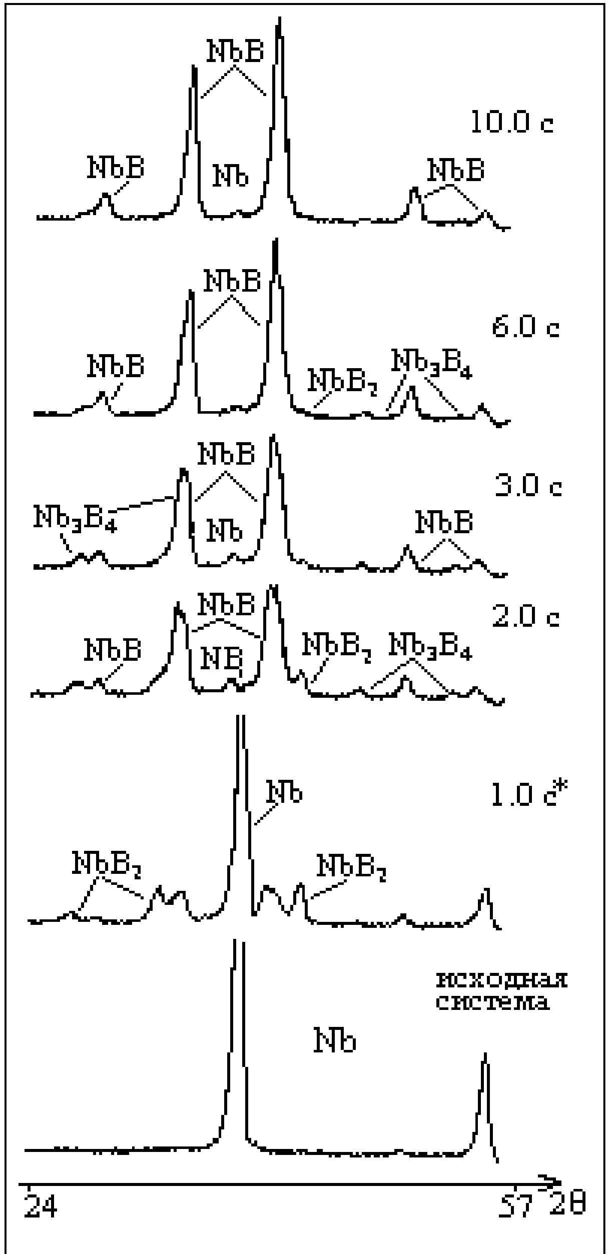

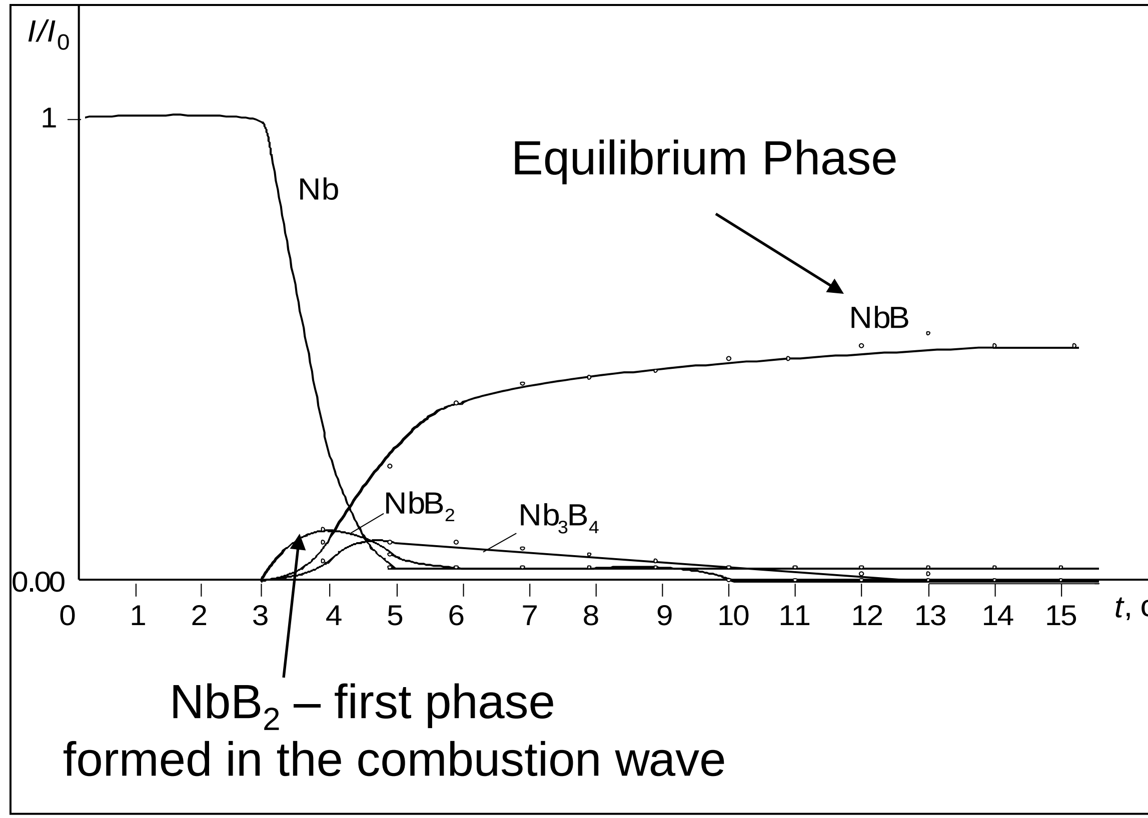

Argonne Laboratory: Advanced Photon Source

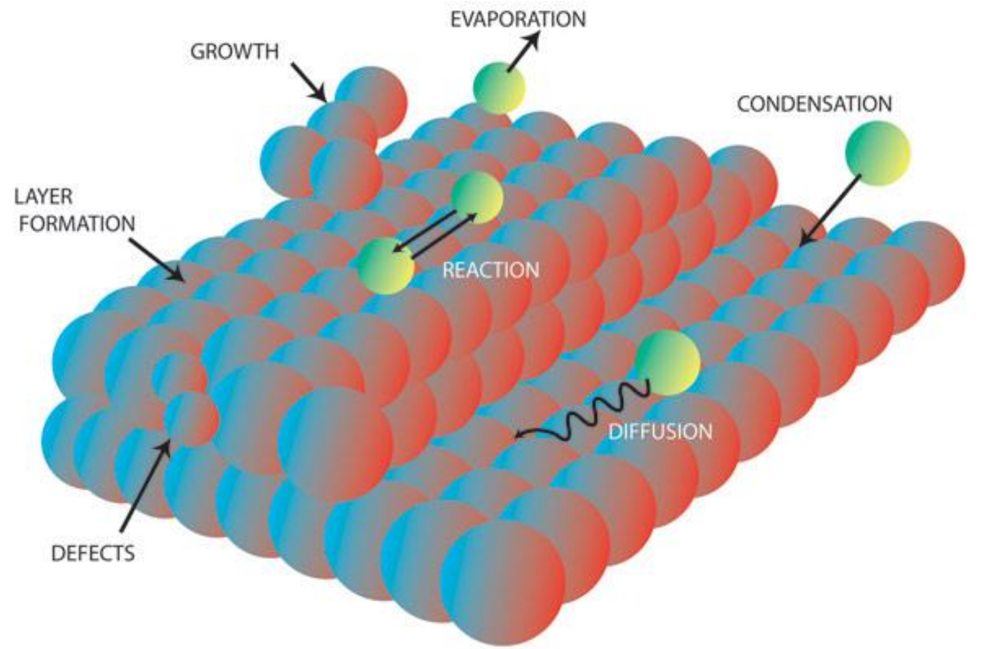

Time resolution: 10^{-12}s
Scale resolution: 1 μm

Collaboration with group leaded by Dr. Jin Wang
Experimental Facilities Division
Argonne National Laboratory

High-Speed Electrothermography

Electrothermography (ETM)

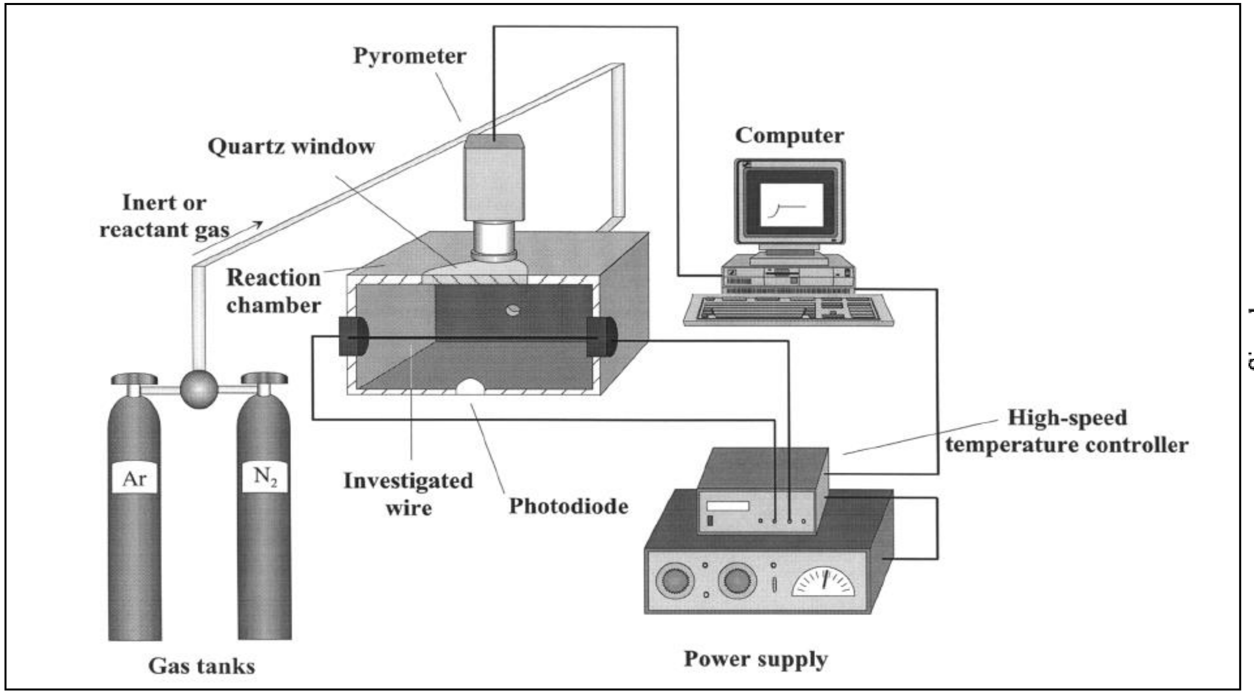

Schematic diagram of the electrothermography setup

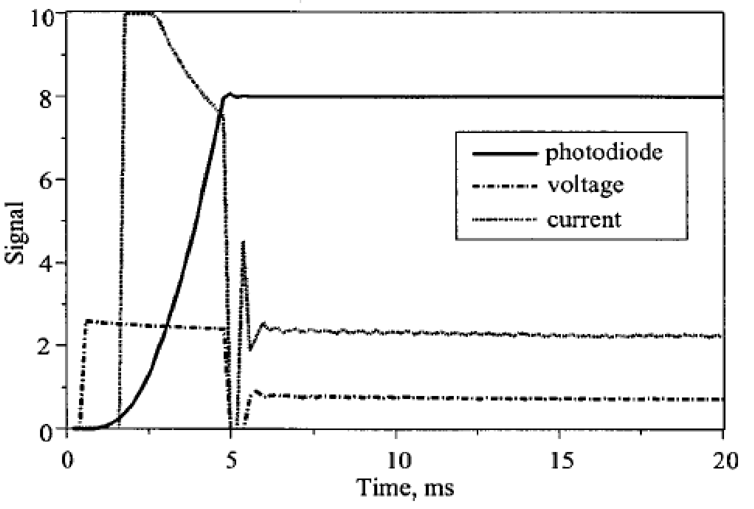

Typical response characteristics of temperature controller

The Concept of ETM

$$\rho c \pi r_0^2 L \frac{dT}{dt} = q + p(t) - h(T), \qquad (1)$$

where *T*—wire temperature, *c*—heat capacity, ρ—density, r_0—wire radius, *L*—wire length, *p*(*t*)—rate of heat generation from electric current (Joule heat), *h*(*T*)—rate of heat loss (mainly by radiation), and *q*=*q*(*t*,*T*, η), the rate of heat evolution, with η being the degree of conversion.

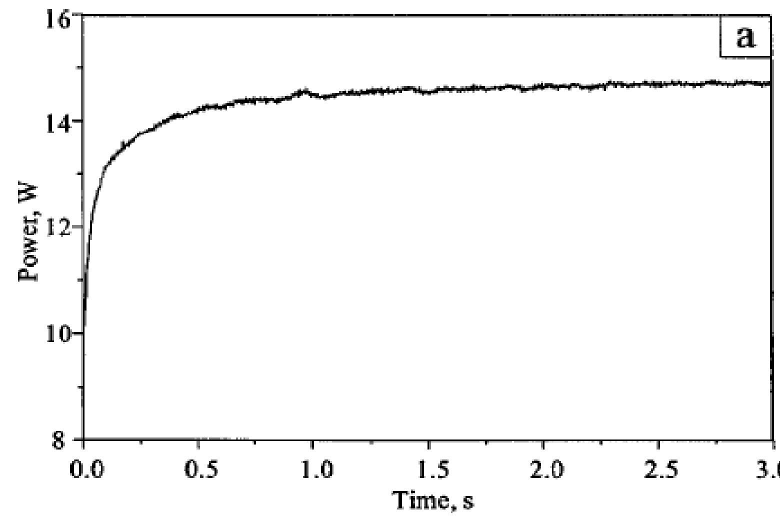

Since *q*(*t*) varies with time as reaction proceeds, the experiment is conducted by varying the electric power *p*(*t*) in order to maintain constant temperature. Under these conditions, from Eq. (1) with *dT*/*dt*=0, we have:

$$q(t)|_T = h(T) - p(t)|_T. \qquad (2)$$

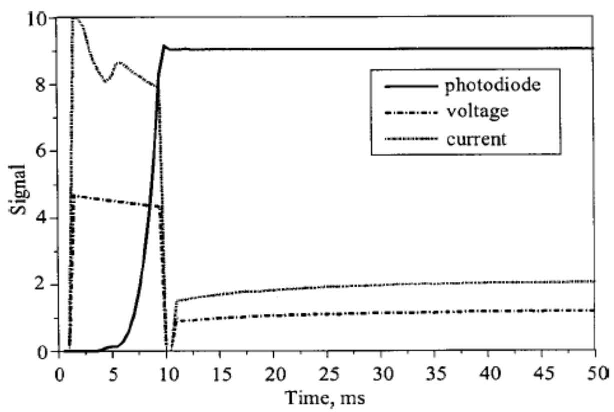

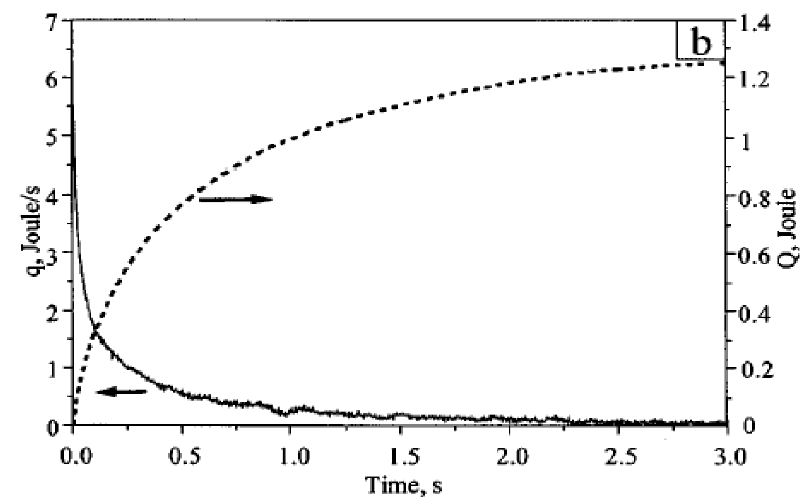

Molybdenum – Silicon System

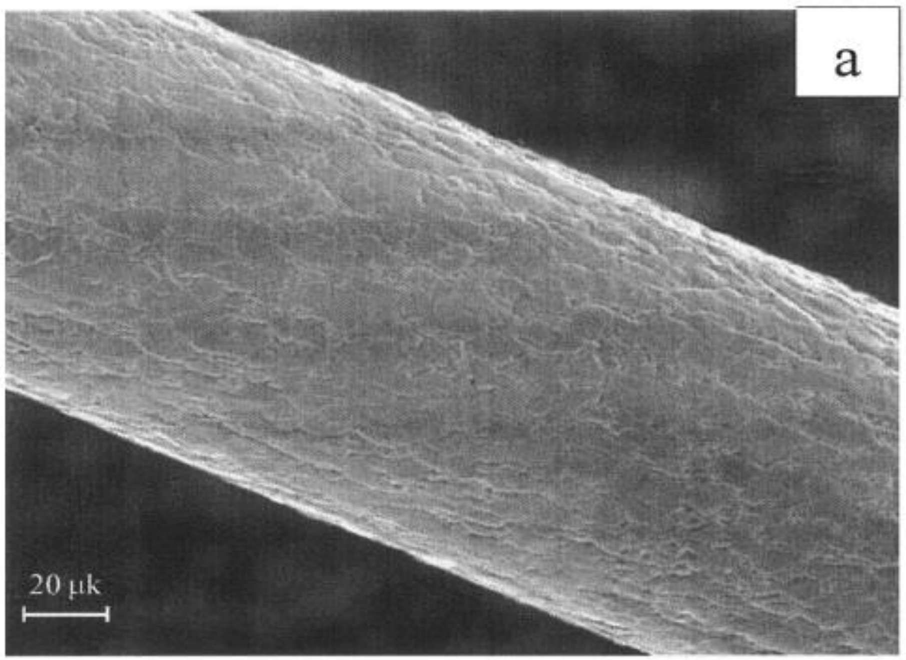

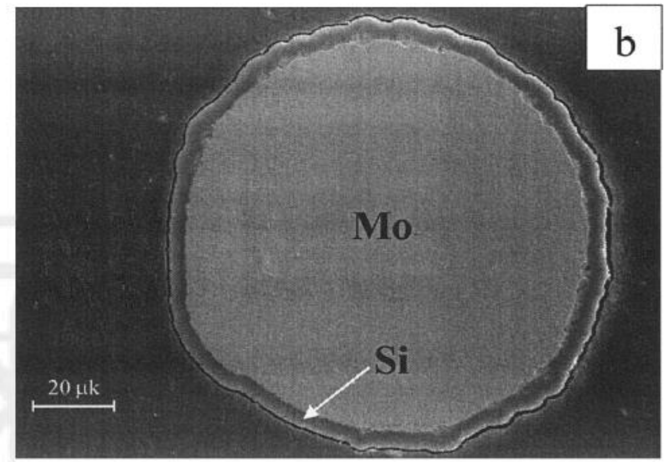

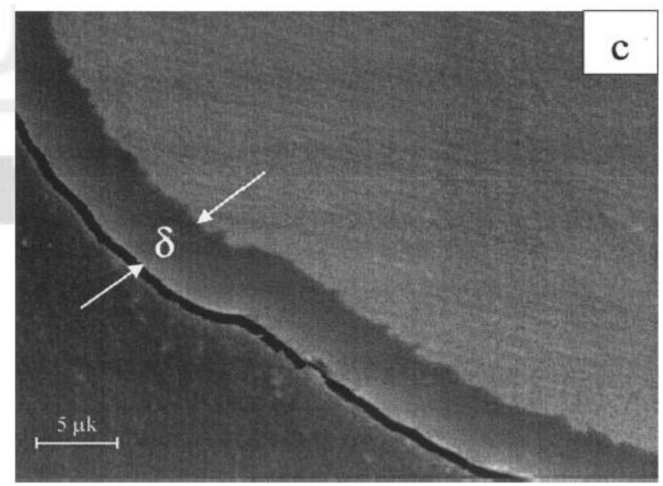

(a) Typical surface, and (b– c) cross section of Mo wire clad by Si

Kinetics of High Temperature Reaction: Mo-Si System

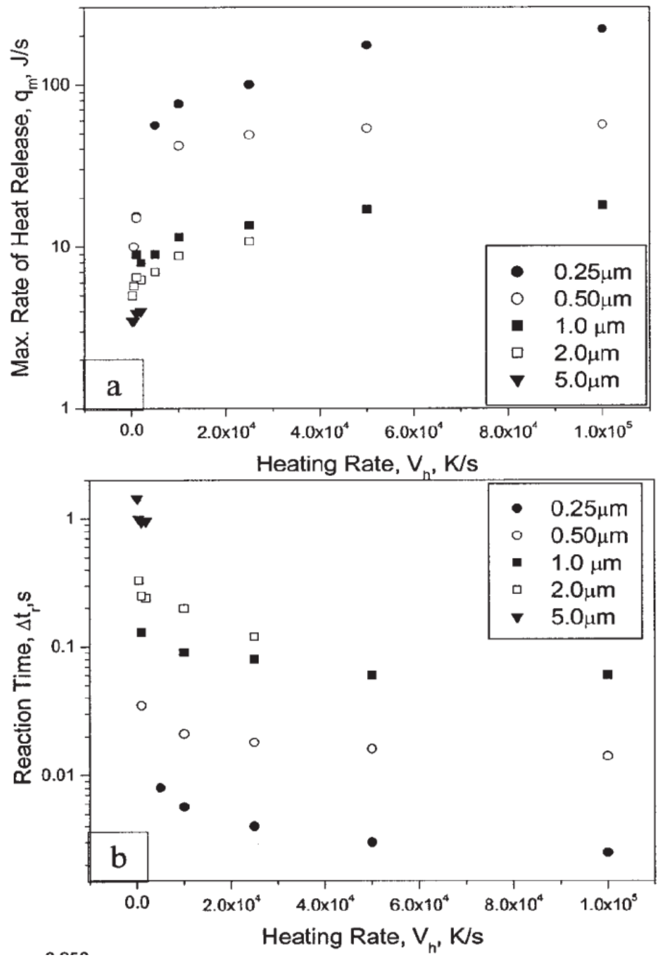

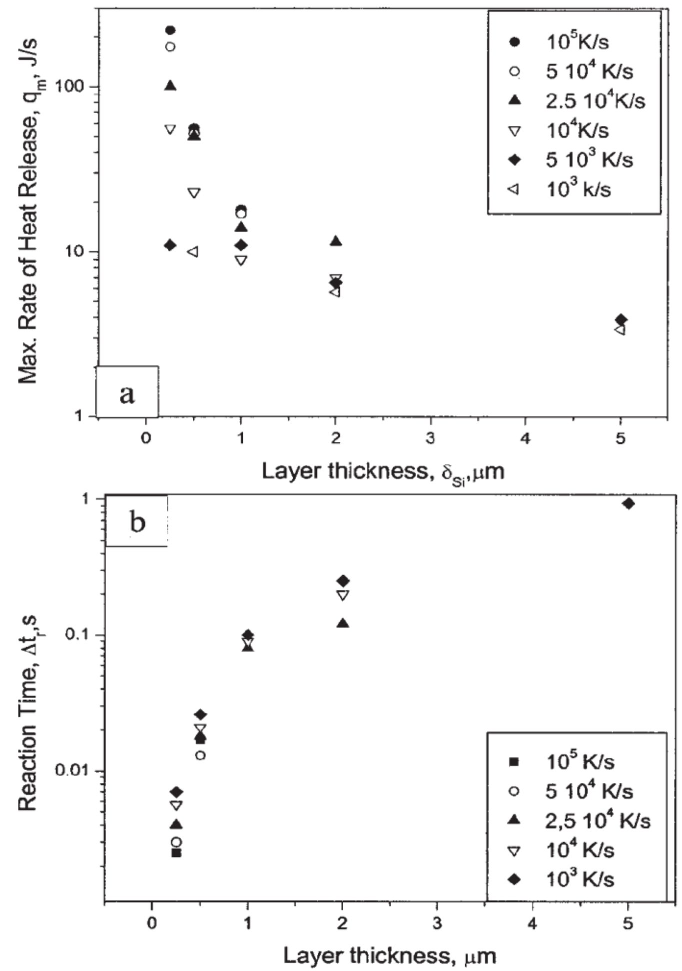

Reaction Mechanisms

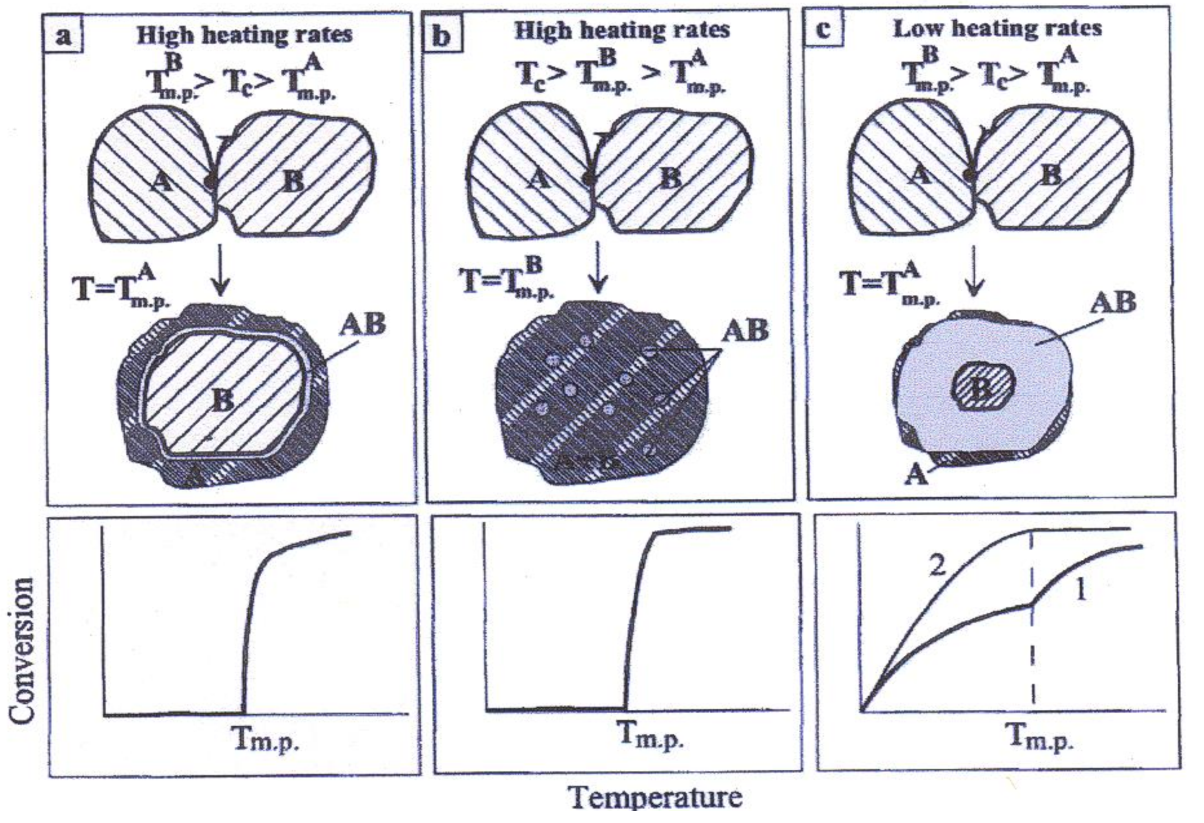

- Diffusion through solid product's layer ~10^{-10} cm^2/s
- Dissolution-recrystallization ~10^{-5} cm^2/s
- Reaction coalescence ~10^{-5} cm^2/s

Electro Thermal Explosion

ETE-100

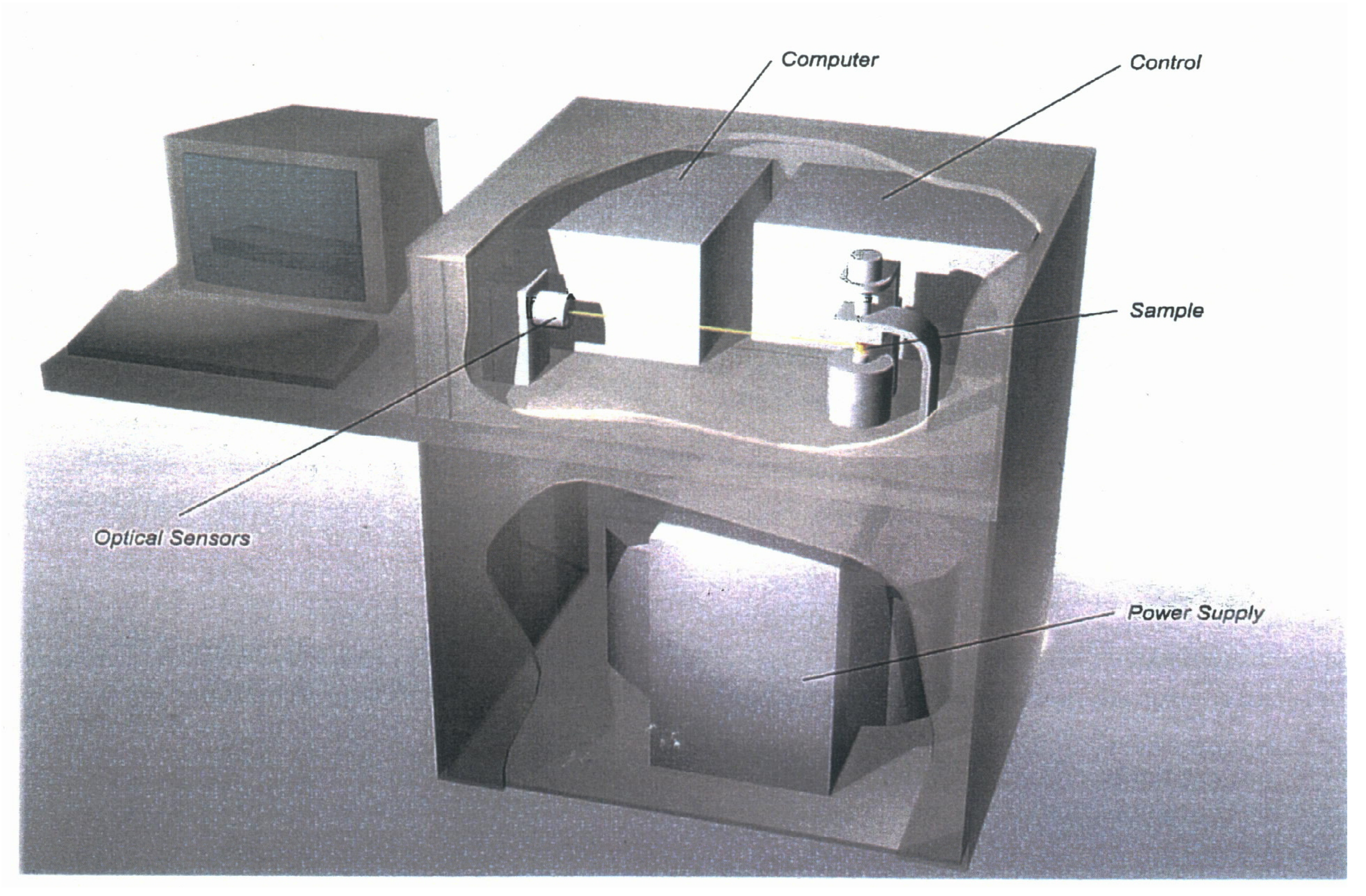

Collaboration with
ALOFT Company Berkley, CA

Office of Naval Research ONR BAA 07-001
Project: FUNDAMENTAL MECHANISMS OF REACTIVE MATERIALS RESPONSE UNDER EXTREME MECHANICAL STIMULATION

Kinetics of Heterogeneous Rapid High-Temperature Reactions

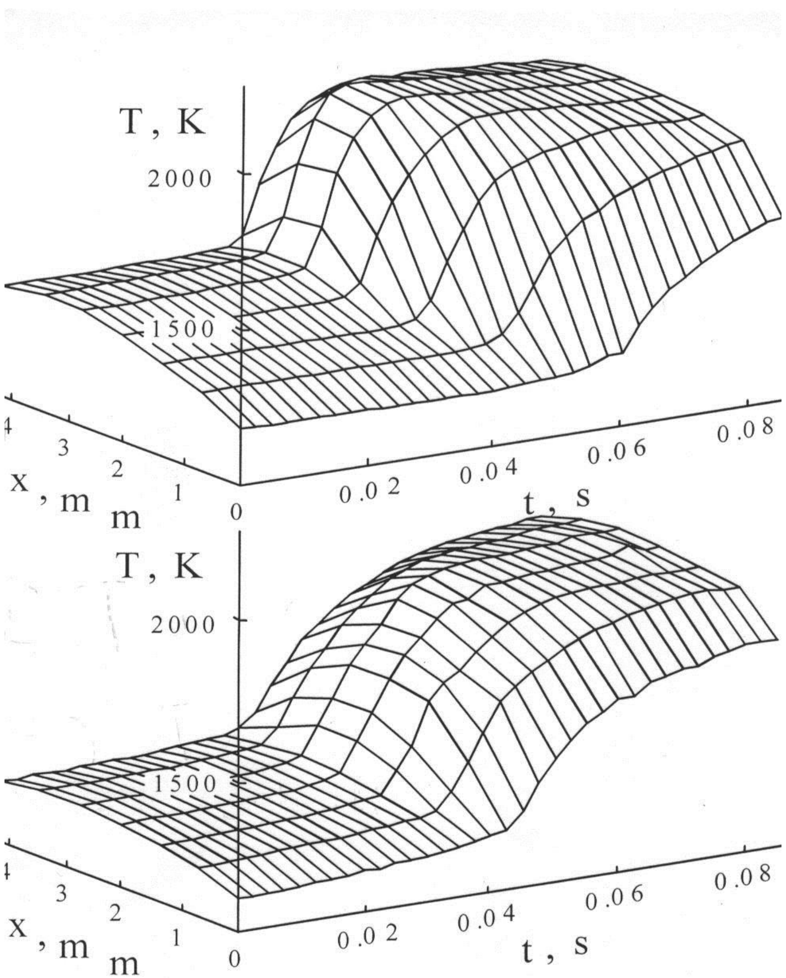

Ni-Al System

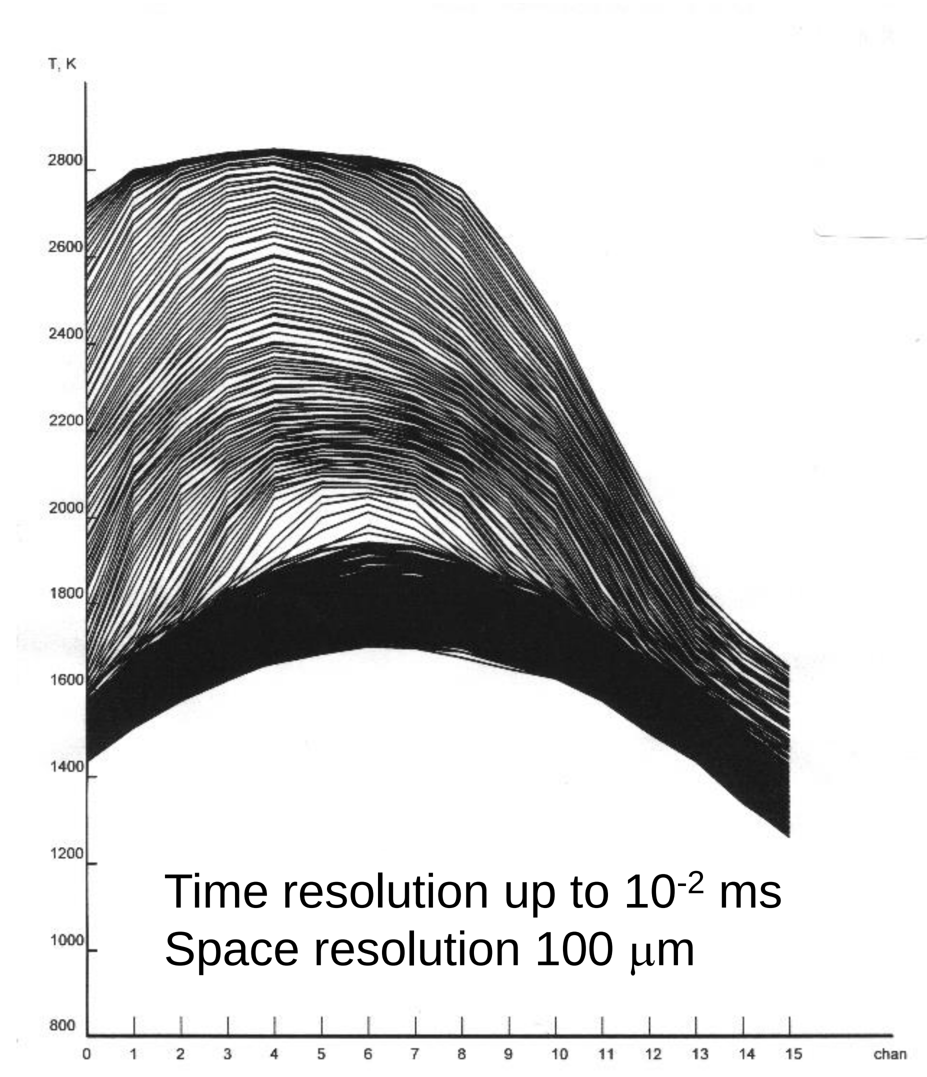

Ti-C System

Self-Sustained Gasless Heterogeneous Reactions:

Additional Technological Capabilities

Joing of Refractory and Dissimilar Materials

Collaboration with Honeywell
Aircraft Landing Systems, South Band, IN

Concept of Reactive Joining

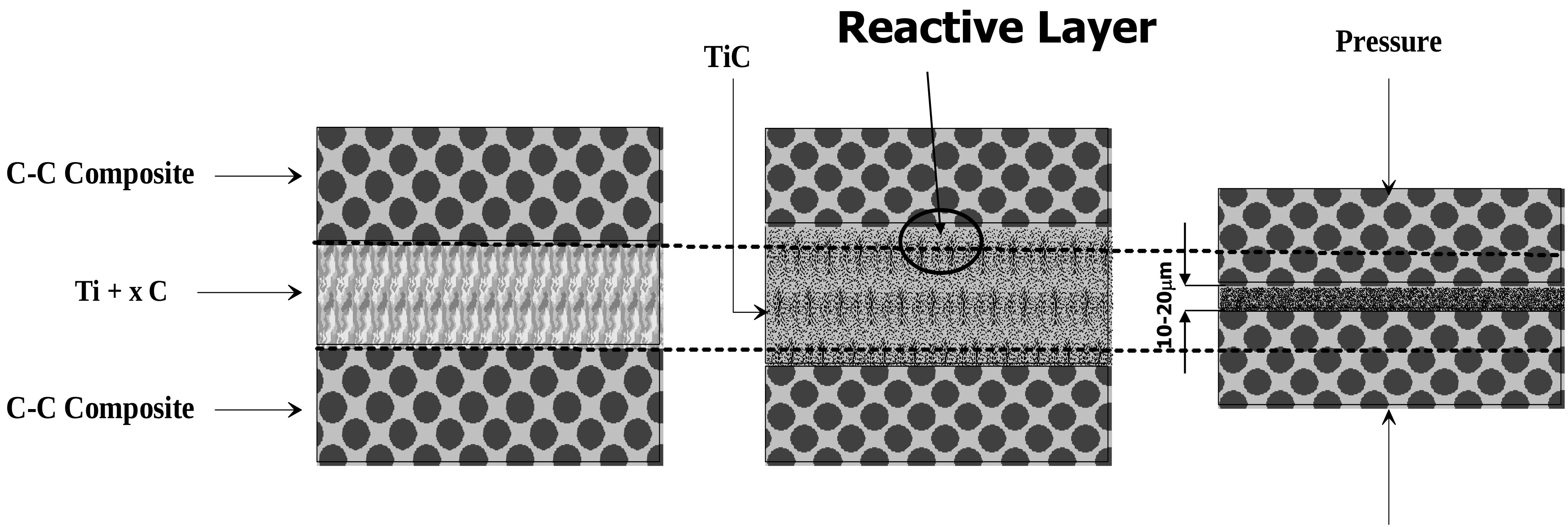

Chemical interaction between C-C composite and reactive media

VCS-RJ of C-C Composites

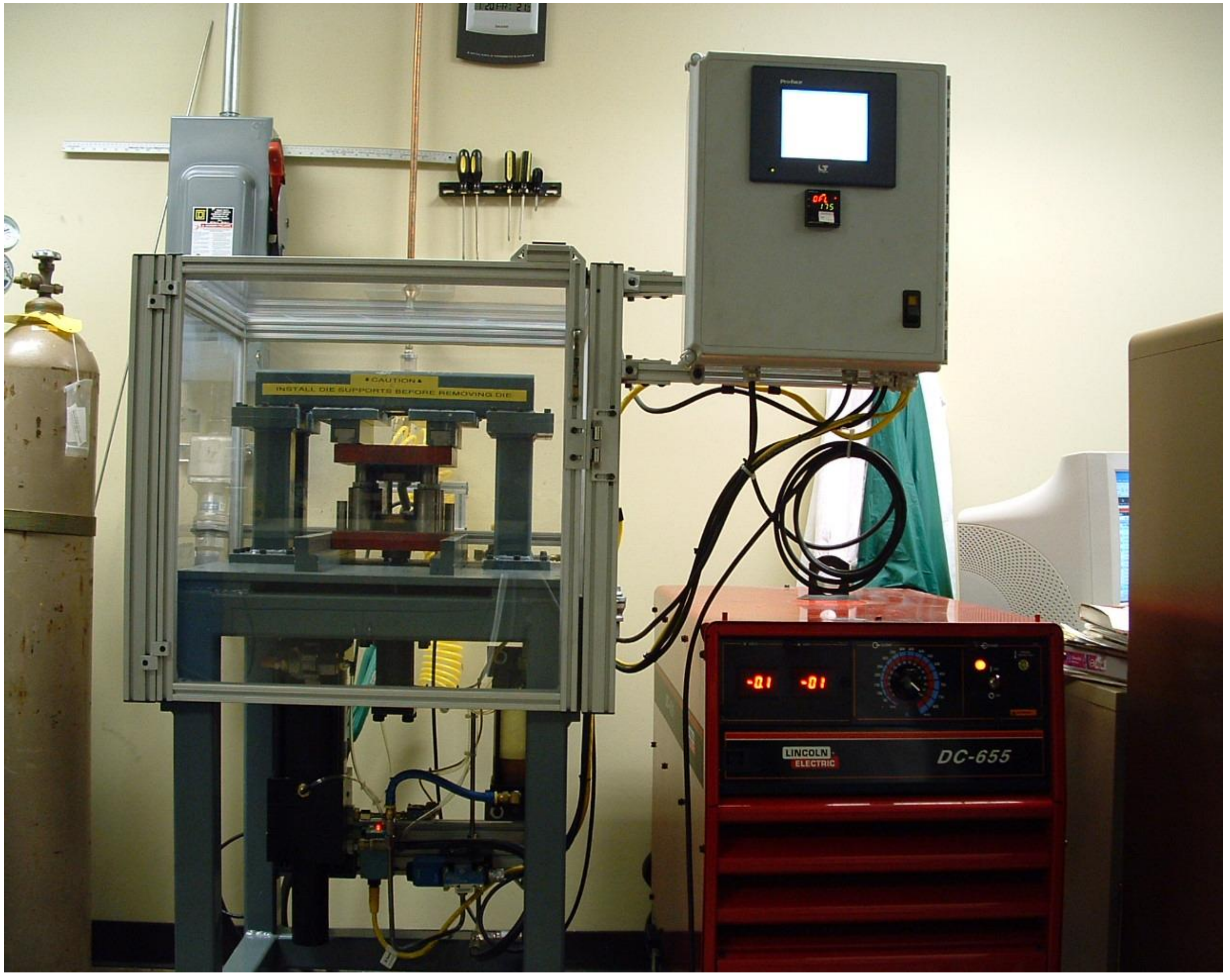

- Max. Current: 950 A
- Max Voltage: 44 V
- Max Load: 35,000 N
- Press Response Time: 10 ms
- Max. Sample diameter: 5”

Typical Microstructure of Joining Layer

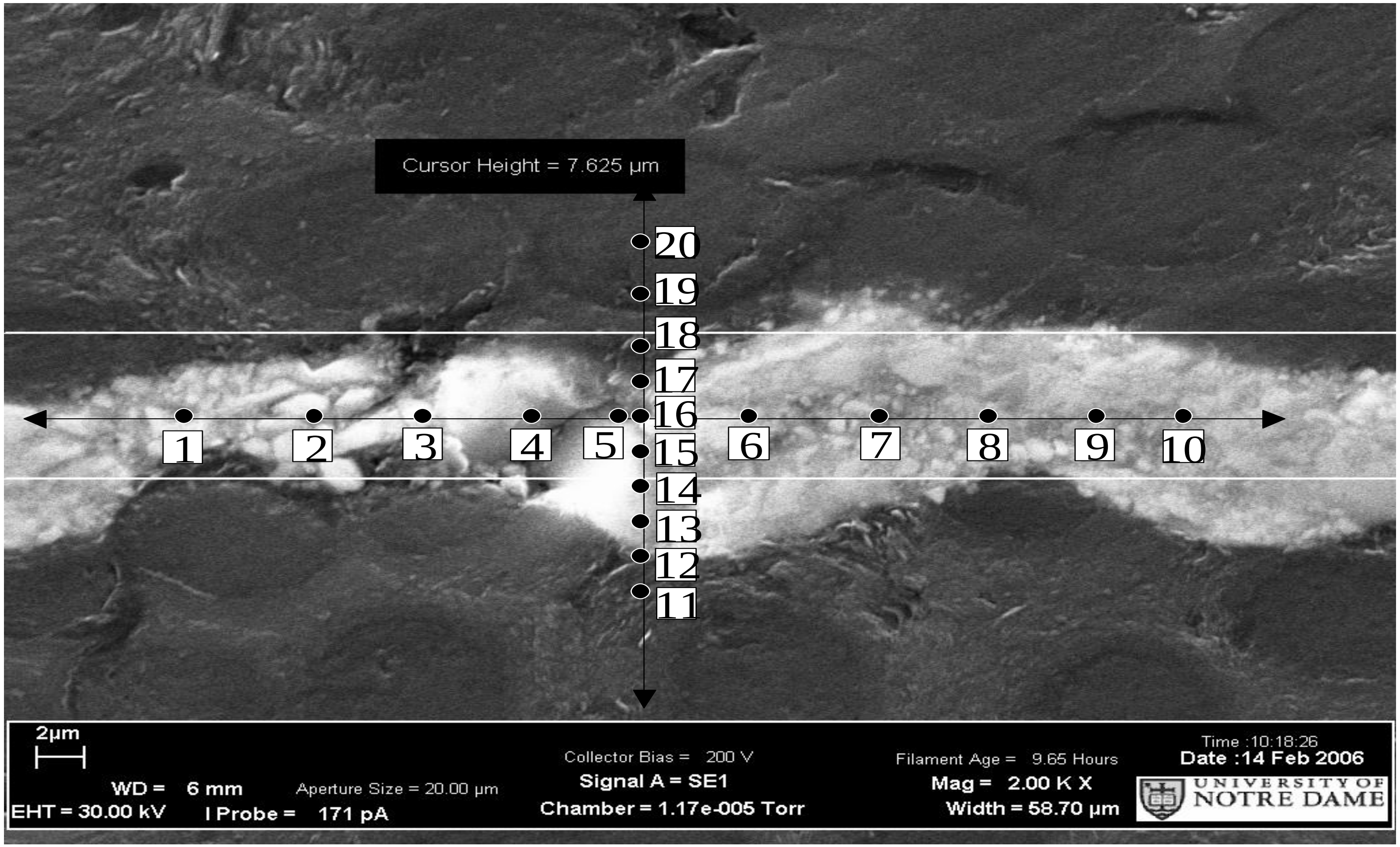

Direction relative to joint layer	Position of EDS analysis									
	Element concentration wt. %; Ti / C									
Along	1	2	3	4	5	6	7	8	9	10
	76.9 / 23.1	78.5 / 21.5	76.7 / 23.3	80.9 / 19.1	78.5 / 21.5	65.5 / 34.5	73.7 / 26.3	68.2 / 31.8	76.0 / 24.0	76.3 / 23.7
Normal	11	12	13	14	15	16	17	18	19	20
	9.0 / 91.0	26.9 / 73.1	58.7 / 41.3	76.2 / 23.8	79.5 / 20.5	81.3 / 18.7	73.0 / 27.0	41.4 / 58.6	21.3 / 78.7	8.2 / 91.8

Scaling Up - Die

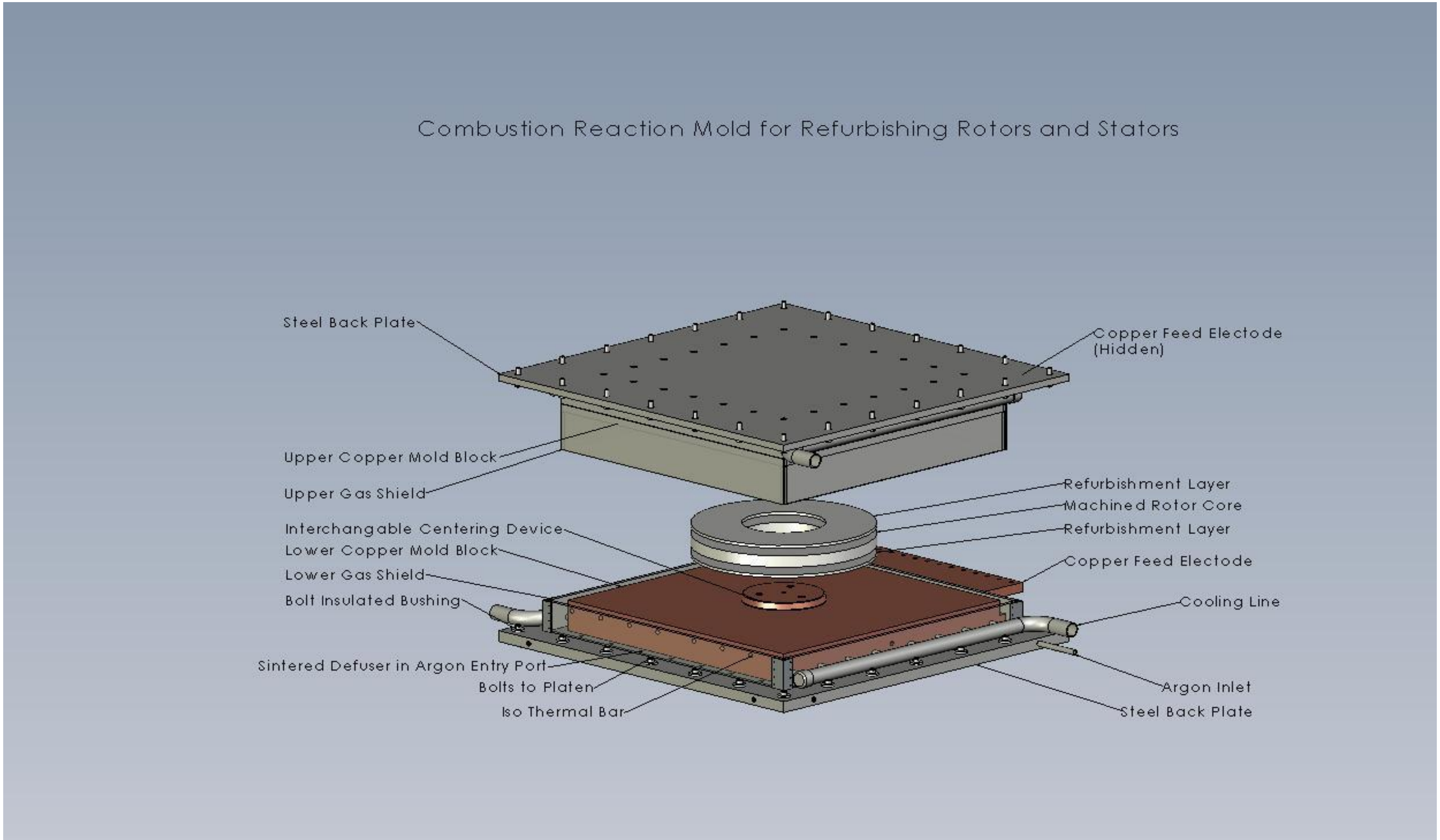

Scaling up - Overview

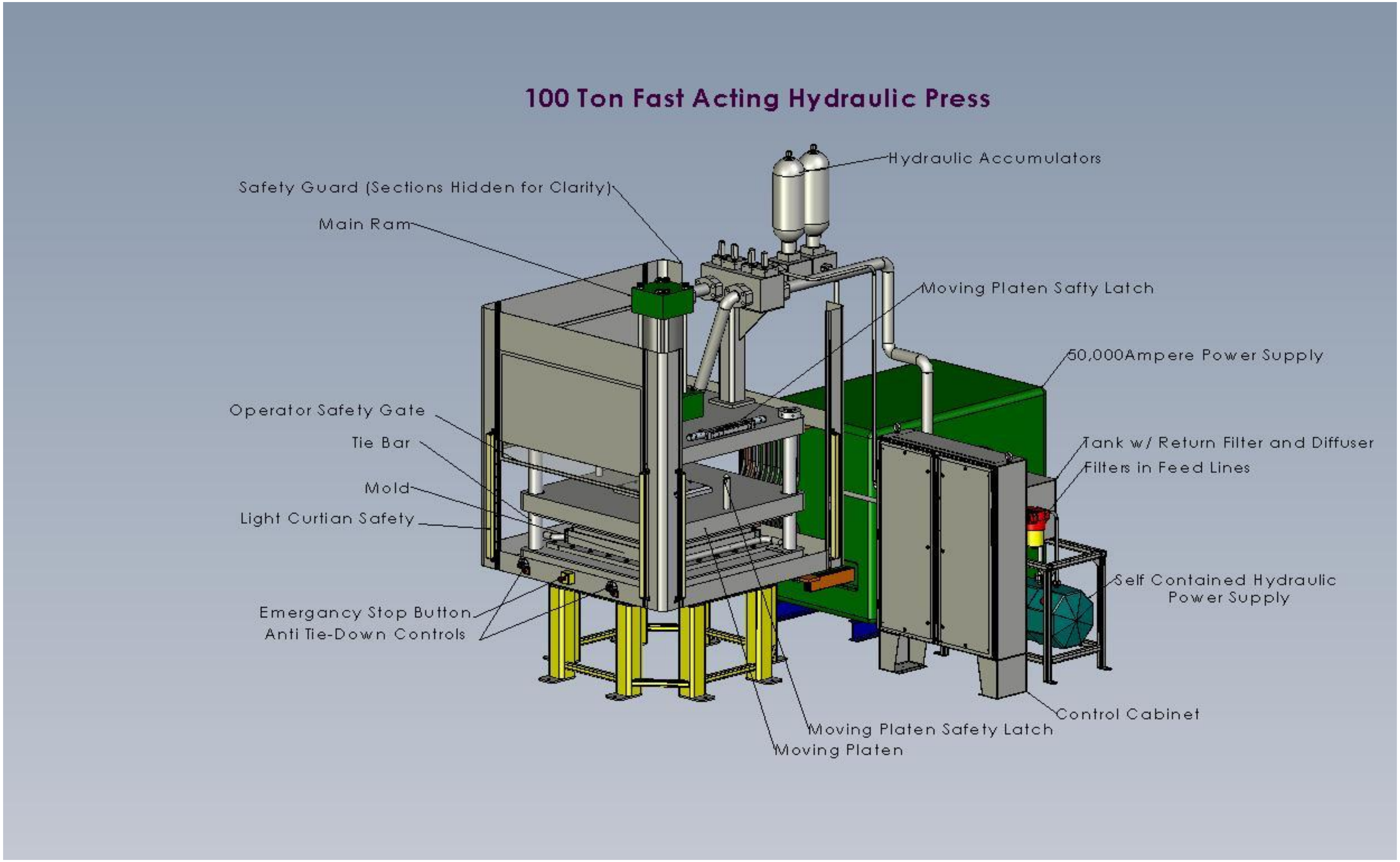

Solution Combustion Synthesis:

Nano Materials

Concept of SCS

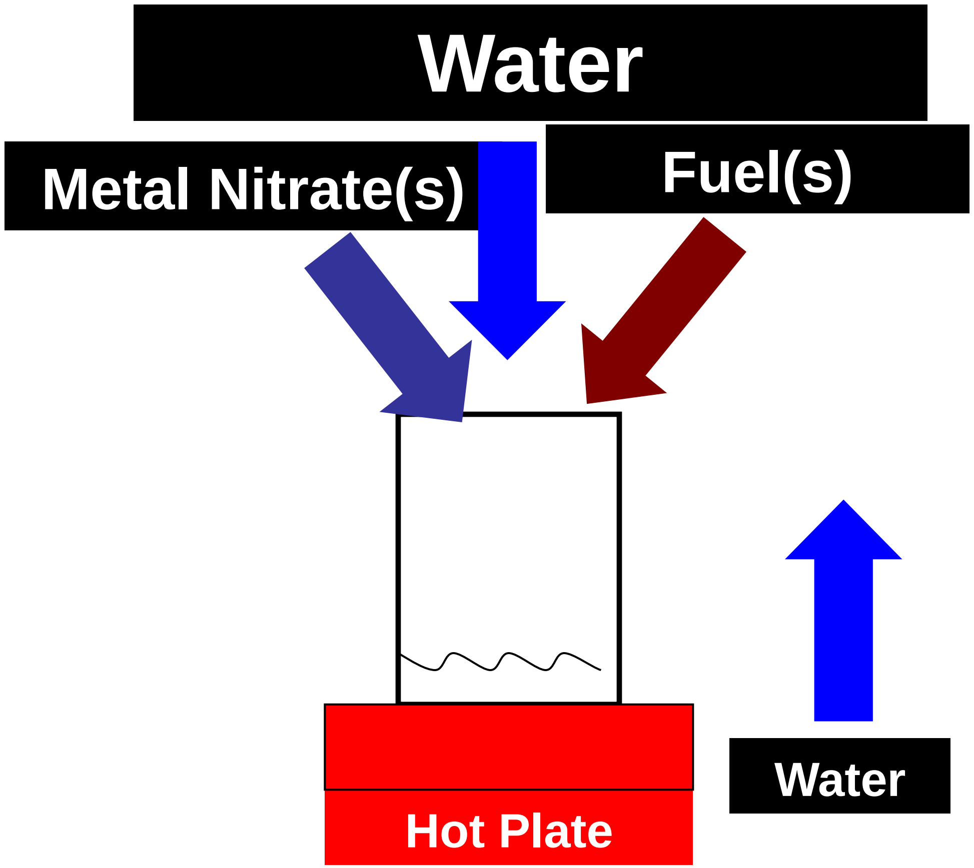

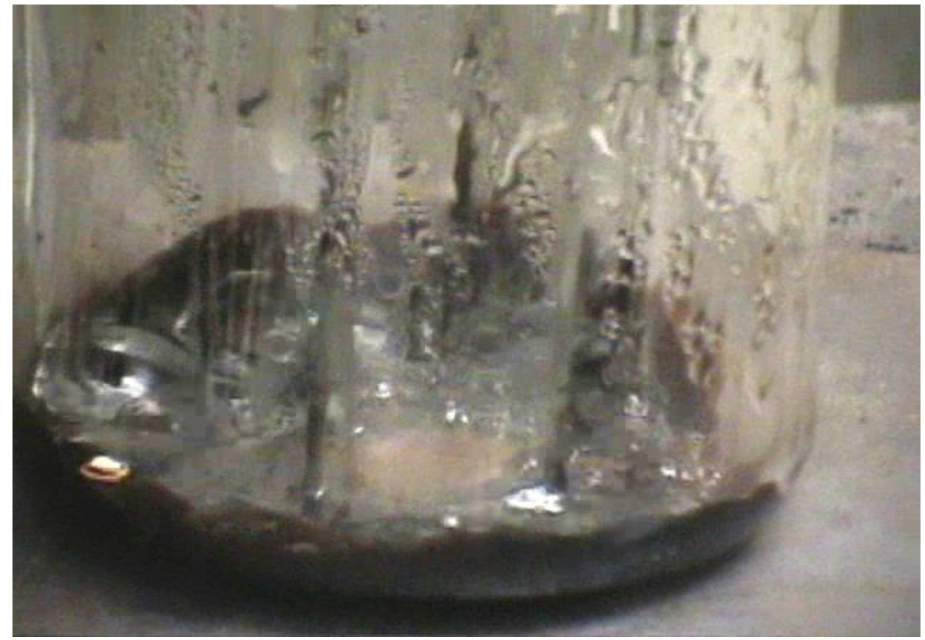

$$Me^{\nu}(NO_3)_{\nu} + (\nu\cdot\phi)\ CH_2NH_2CO_2H + \nu\cdot(\phi-1)\ O_2 \Rightarrow$$
$$MeO_{\nu/2}(s) + (\nu\cdot\phi)CO_2(g) + \phi\ H_2O(g) + \nu\cdot(\phi+1)/2\ N_2(g)$$

where Me^{ν} is a metal with valence ν; ϕ is a fuel to oxidizer ratio, $\phi = 1$ means that the initial mixture does not require atmospheric oxygen for complete oxidation of fuel, while $\phi > 1$ (< 1) implies fuel-rich (lean) conditions.

Reactants mixed on the molecular level !!

Solution Combustion: Volume Reaction Mode

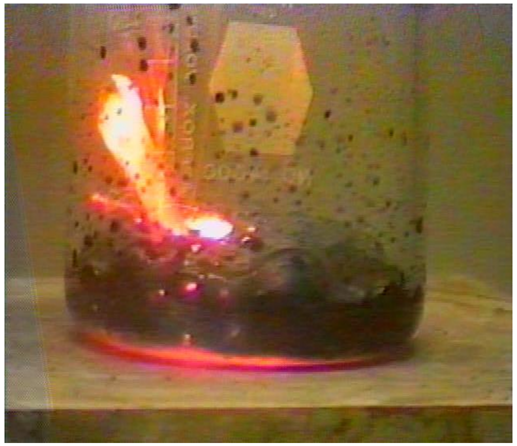

Self-ignition

Volume reaction

Product

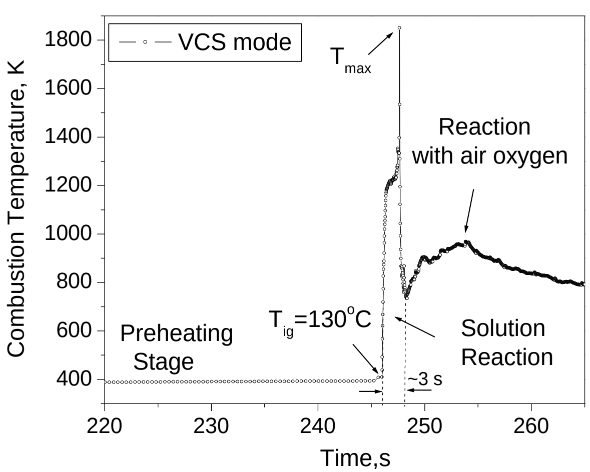

- Reactants mixed on the molecular level
- Short reaction time (~seconds)

***Nano*-size particles**

- Relatively high temperatures

Well *crystalline* structure
Avoid *calcination* !!

VCS: Different Fuels

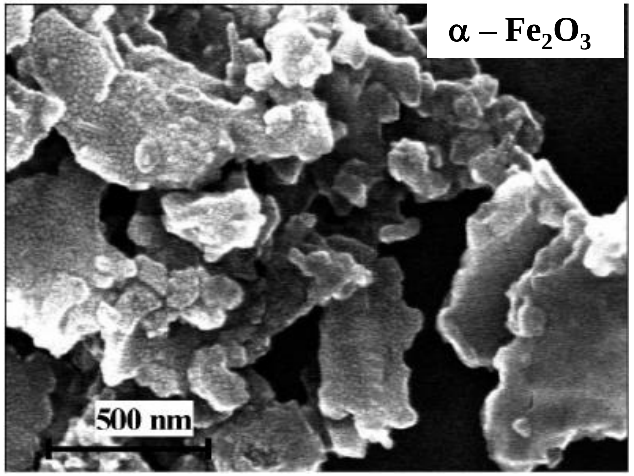

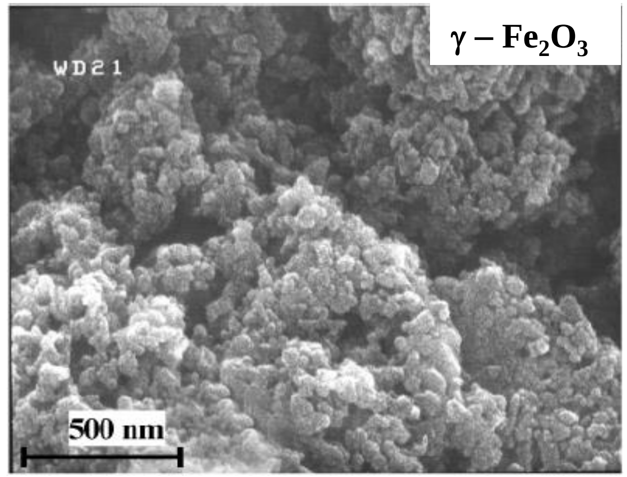

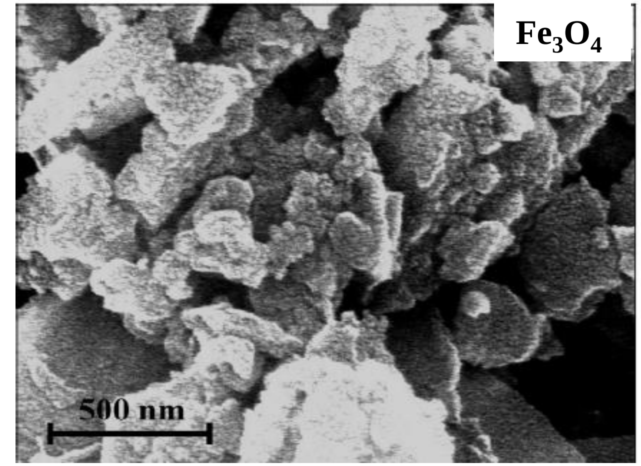

Table 2. Phase Composition and Surface Area for the Hydrazine–Iron Nitrate System

ϕ	phase composition	surface area, m^2/g
0.34	amorphous	125
1	$(\gamma+\alpha)$-Fe_2O_3	52
2.0	$(\gamma+\alpha)$-Fe_2O_3	65
2.2	$(\gamma+\alpha)$-Fe_2O_3	50
3	γ-Fe_2O_3	28

Table 4. Phase Composition and Surface Area for the Citric Acid–Iron Nitrate System

ϕ	phase composition	surface area, m^2/g
1	α-Fe_2O_3	35
1.2	α-Fe_2O_3	45
1.4	α-Fe_2O_3	42
3	α-Fe_2O_3	30

Table 5. Phase Composition and Surface Area for Different Fuels and Iron Nitrate in Argon

fuel	surface area, m^2/g	composition
glycine	4	Fe_3O_4
hydrazine	42	$(\alpha+\gamma)$-Fe_2O_3
citric acid	45	Fe_3O_4

Deshpande K., Mukasyan A.S. and Varma A., Chem. Mater. 16 (24), 4896-4904 (2004)

Example: Synthesis of Iron Oxides

Conditions	Phase	Surface area, m^2/g
Iron nitrate, glycine and hydrazine	α Fe_2O_3	60
Iron Oxalate, ammonium nitrate and hydrazine	γ Fe_2O_3	200
Iron nitrate and citric acid in argon	Fe_3O_4	50

Solution Combustion:
Thermal Explosion Mode

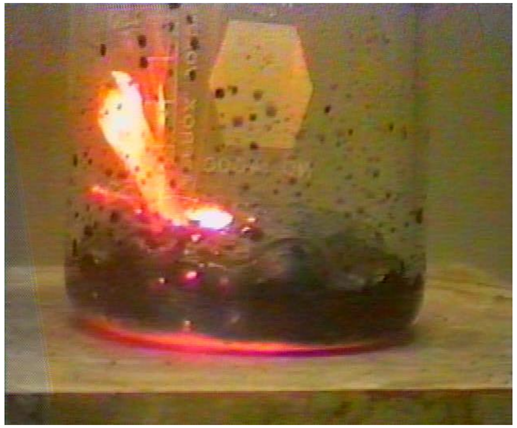

Self-ignition

Volume reaction

Product

COMBUSTION PROCESS = BLACK BOX

THERMAL EXPLOSION =DIFFICULT TO CONTROL

Solution Combustion:

Sol-Gel Self-Propagating Mode

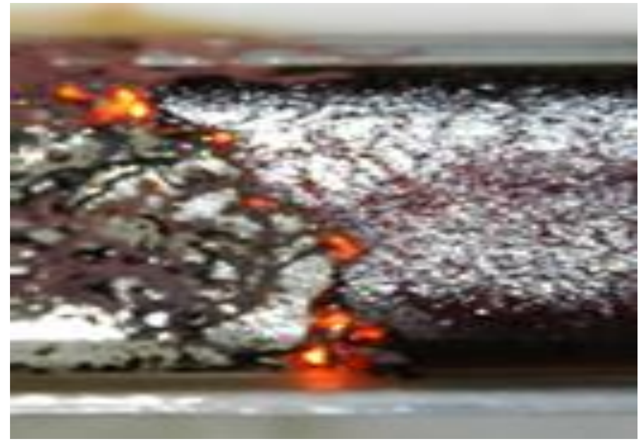

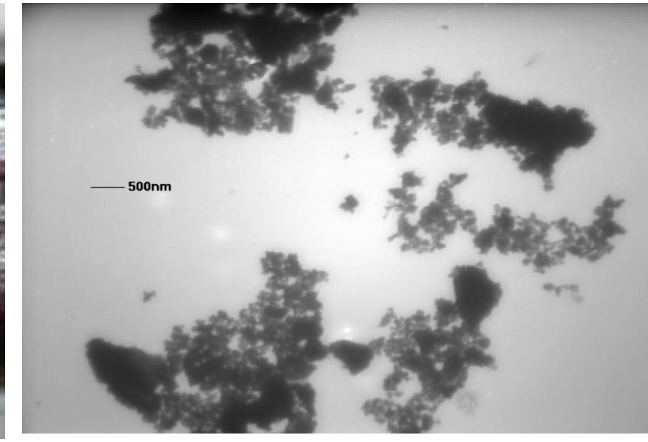

Direction of reaction front propagation

Product

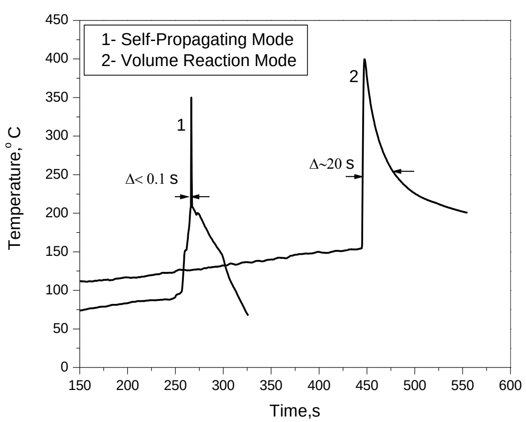

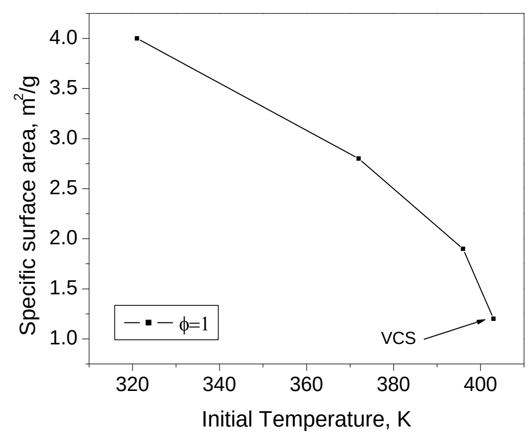

- Easy to control
- Product quenching effect
- 10-15 nm particles

Mukasyan, A., P.Epstein and P.Dinka, Proc. Combustion Institute, 31(2), 1789-1795 (2007)

Solution Combustion:
Impregnated Combustion Mode

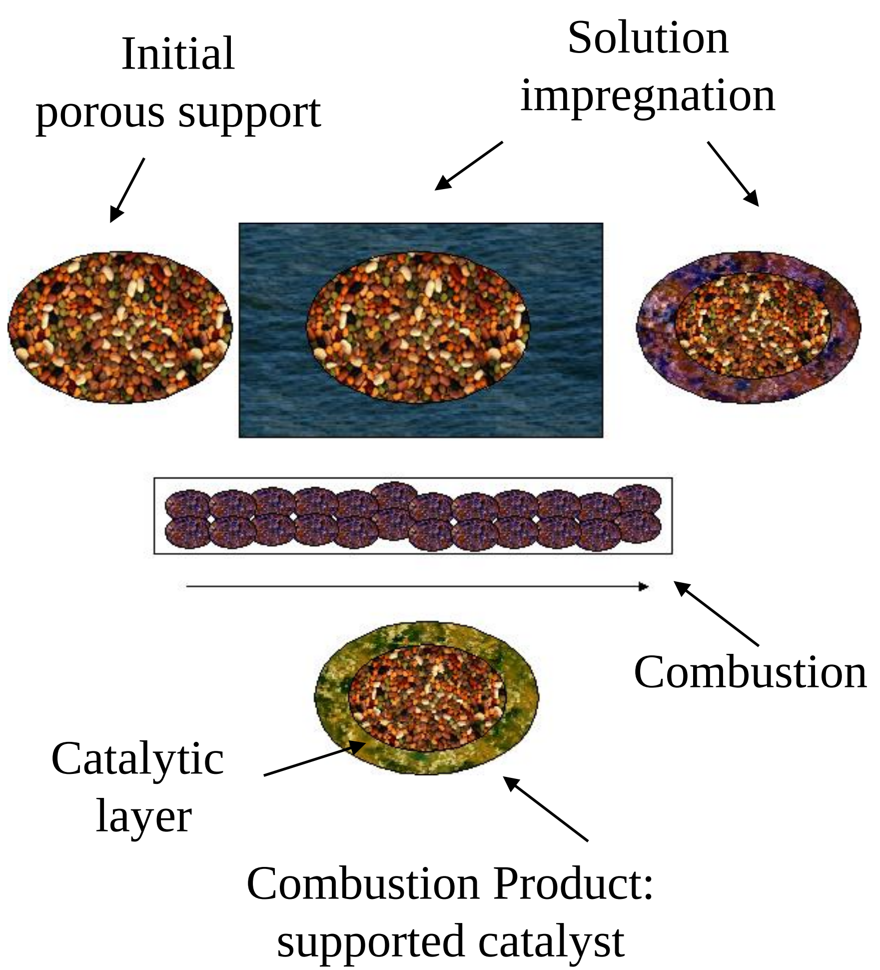

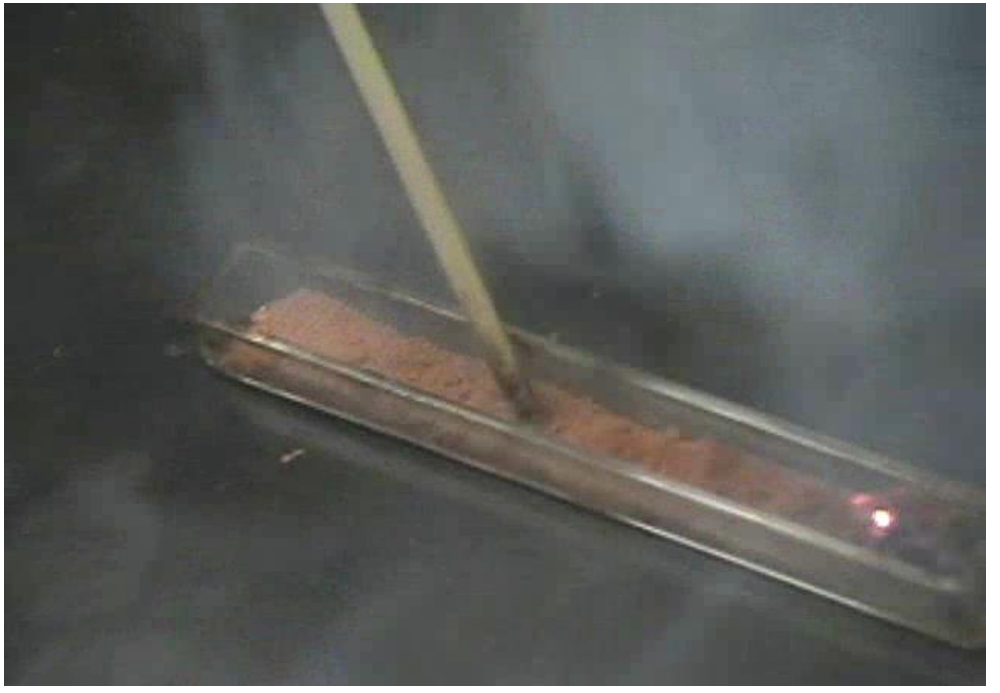

- Very high specific surface area of active sites
- High mechanical properties

Dinka P. and Mukasyan A., J. Phys. Chem. 109(46), 21627-21633 (2005)

Nano-Reactor Effect !!

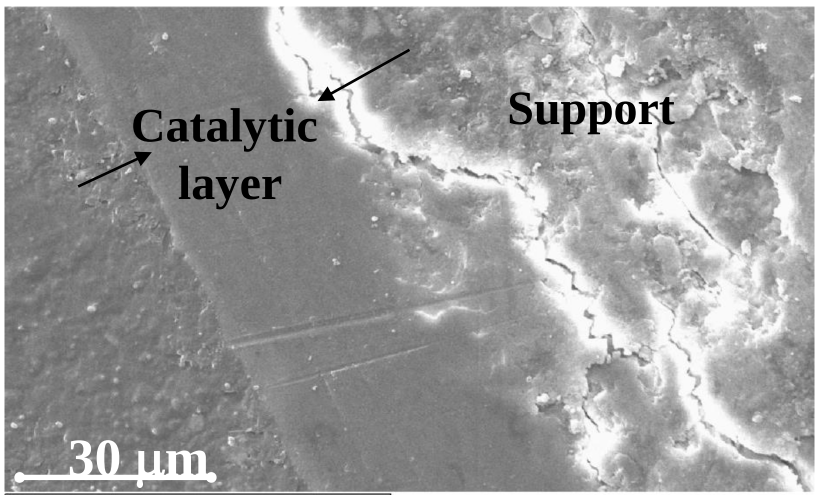

Support	BET support [m^2/g]	BET iron oxide powder [m^2/g]	BET of supported catalyst [m^2/g]
Al_2O_3 activ.	**149**	40	**225**
α -Al_2O_3	5.1	4.5	5.8
γ - Al_2O_3	244	37	197
ZrO_2	125	22	112

Dinka P. and Mukasyan A., J. Phys. Chem. 109(46), 21627-21633 (2005)

Solution Combustion:

Impregnated Paper

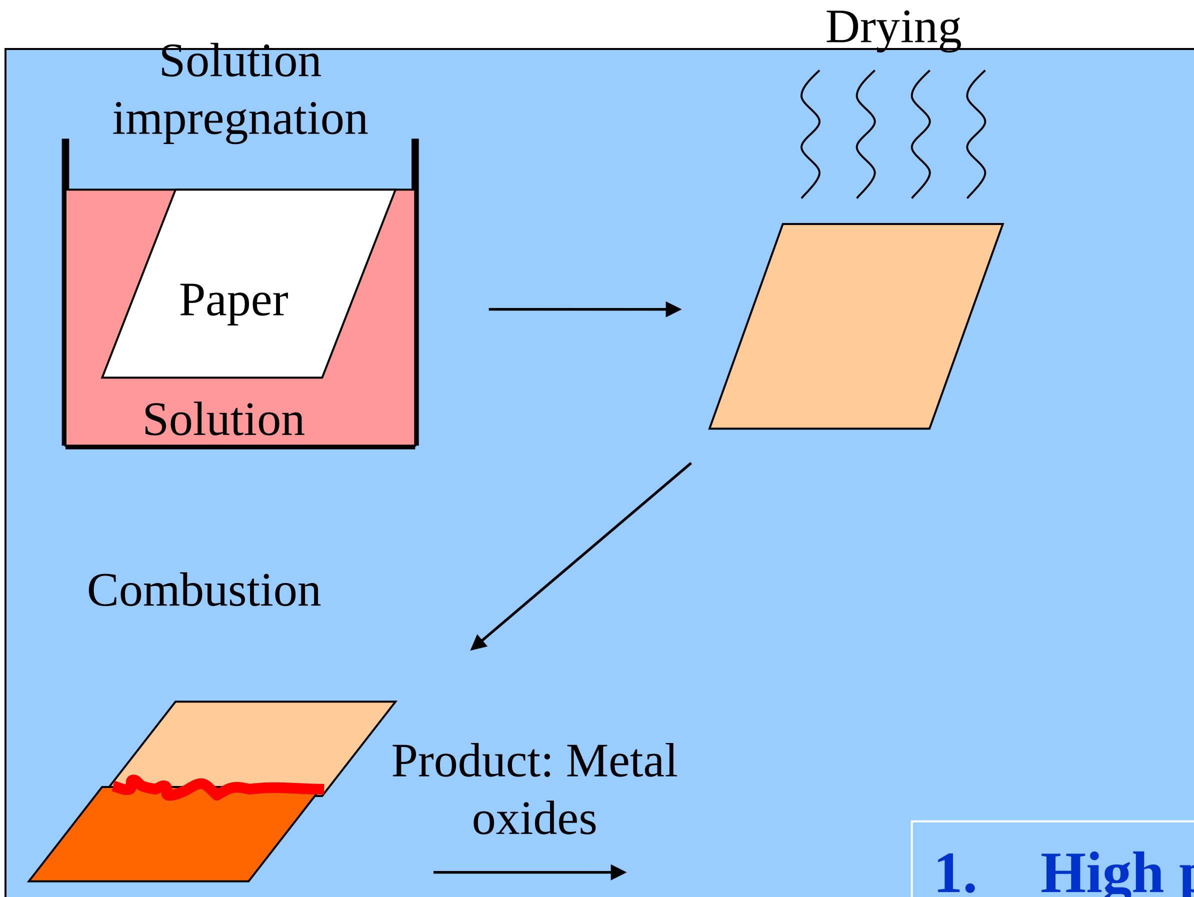

1. **High product yield**
2. **Reactions in low exothermic systems**
3. **Continuous technology**

Mukasyan, A.S, Dinka, P. J. Adv. Eng. Mater. 9, 653-657. (2007)

Continuous Technology
for Synthesis of Nanopowders

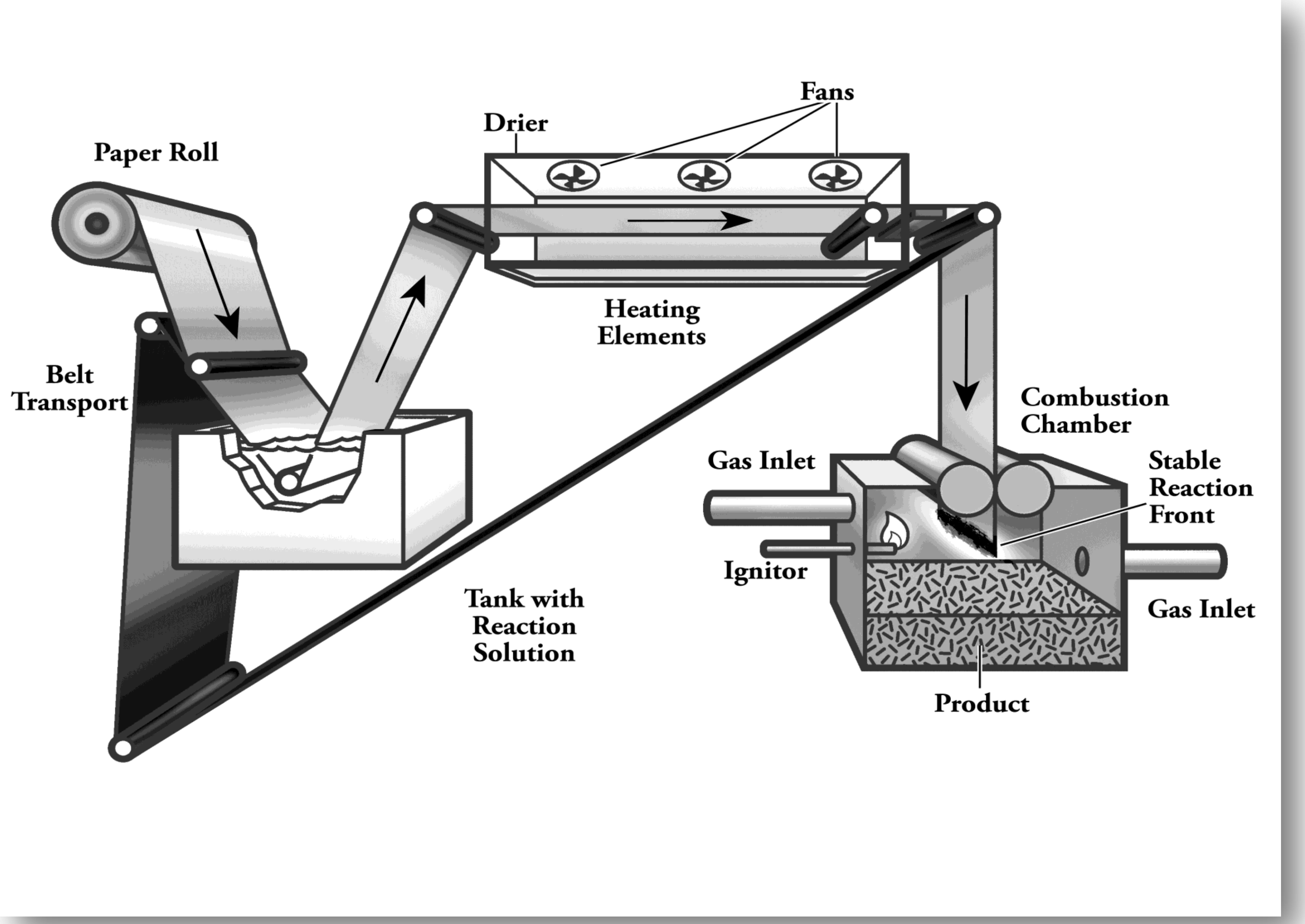

Continuous Technology
for Synthesis of Nanopowders

- Production capacity: 15 – 500 g/h
- Safe process
- Low energy consumption

Mukasyan A., Dinka, P., US Patent US2006/030486, Filed: August 4, 2006.

Perovskites by SC

B-site: $Fe_{(1-Y)}MY$*	A-site: $La_{(1-X)}Sr_X$	A-site: $Ce_{(1-X)}Sr_X$	A-site: $La_{(1-X)}Ce_X$
	X=0.4	X=0.4	X=0.4
Y=0	$La_{0.6}Sr_{0.4}FeO_3$	$Ce_{0.6}Sr_{0.4}FeO_3$	$La_{0.6}Ce_{0.4}FeO_3$
M: Ni Y=0.2, 0.4, 0.6	$La_{0.6}Sr_{0.4}Fe_{0.8}Ni_{0.2}O_3$ $La_{0.6}Sr_{0.4}Fe_{0.6}Ni_{0.4}O_3$ $La_{0.6}Sr_{0.4}Fe_{0.4}Ni_{0.6}O_3$	$Ce_{0.6}Sr_{0.4}Fe_{0.8}Ni_{0.2}O_3$ $Ce_{0.6}Sr_{0.4}Fe_{0.6}Ni_{0.4}O_3$ $Ce_{0.6}Sr_{0.4}Fe_{0.4}Ni_{0.6}O_3$	$La_{0.6}Ce_{0.4}Fe_{0.8}Ni_{0.2}O_3$ $La_{0.6}Ce_{0.4}Fe_{0.6}Ni_{0.4}O_3$ $La_{0.6}Ce_{0.4}Fe_{0.4}Ni_{0.6}O_3$
M: Co Y=0.2, 0.4, 0.6	$La_{0.6}Sr_{0.4}Fe_{0.8}Co_{0.2}O_3$ $La_{0.6}Sr_{0.4}Fe_{0.6}Co_{0.4}O_3$ $La_{0.6}Sr_{0.4}Fe_{0.4}Co_{0.6}O_3$	$Ce_{0.6}Sr_{0.4}Fe_{0.8}Co_{0.2}O_3$ $Ce_{0.6}Sr_{0.4}Fe_{0.6}Co_{0.4}O_3$ $Ce_{0.6}Sr_{0.4}Fe_{0.4}Co_{0.6}O_3$	$La_{0.6}Ce_{0.4}Fe_{0.8}Co_{0.2}O_3$ $La_{0.6}Ce_{0.4}Fe_{0.6}Co_{0.4}O_3$ $La_{0.6}Ce_{0.4}Fe_{0.4}Co_{0.6}O_3$
	X=0	X=0	X=0
Y=0	$LaFeO_3$	$CeFeO_3$	
M: Ni Y=0.2, 0.4, 0.6	$LaFe_{0.8}Ni_{0.2}O_3$ $LaFe_{0.6}Ni_{0.4}O_3$ $LaFe_{0.4}Ni_{0.6}O_3$	$CeFe_{0.8}Ni_{0.2}O_3$ $CeFe_{0.6}Ni_{0.4}O_3$ $CeFe_{0.4}Ni_{0.6}O_3$	
M: Co Y=0.2, 0.4, 0.6	$LaFe_{0.8}Co_{0.2}O_3$ $LaFe_{0.6}Co_{0.4}O_3$ $LaFe_{0.4}Co_{0.6}O_3$	$CeFe_{0.8}Co_{0.2}O_3$ $CeFe_{0.6}Co_{0.4}O_3$ $CeFe_{0.4}Co_{0.6}O_3$	

High Throughput Apparatus for Catalytic Activity Evaluation

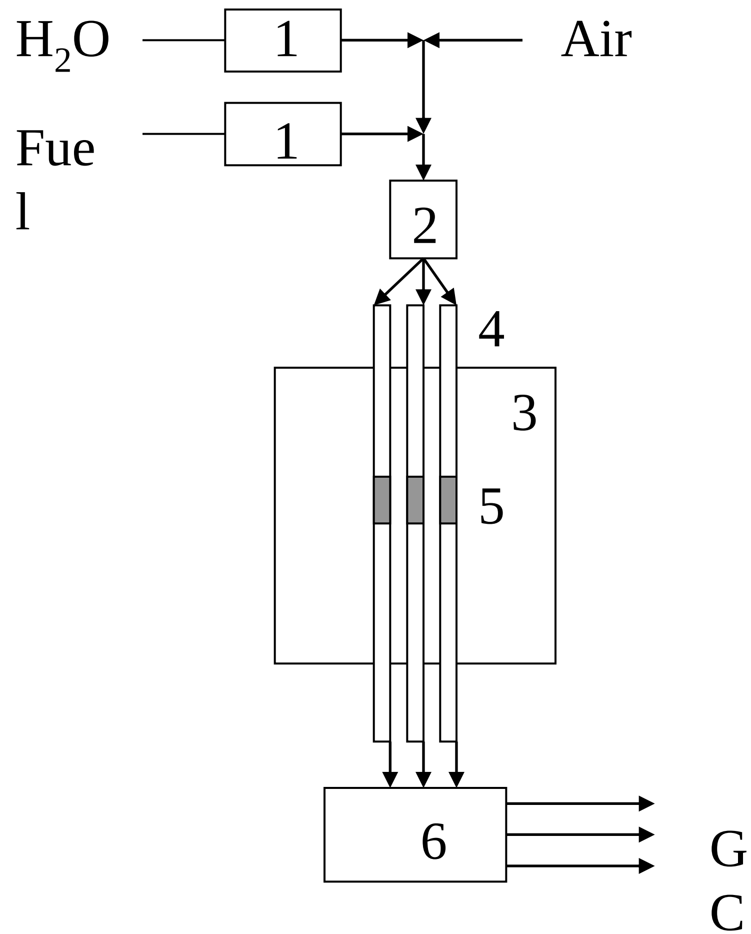

1 – Evaporator
2 – Distribution block
3 – Oven
4 – Reactor set (8 reactors)
5 – Catalysts
6 – Condenser

Reaction conditions: temperature: 800° C, GHSV: 130000 h^{-1}, Fuel: JP-8 surrogate, 10 ppm of sulfur, $H_2O/C = 3$, $O_2/C = 0.35$

Dinka P. and Mukasyan A., *J. Power Sources, 167, 472-481 (2007)*

Auto-thermal Reforming of JP-8 Fuel to Produce Hydrogen

Product gas composition and fuel conversion (steam reforming of JP-8 surrogate with 10 ppm of sulfur on ISC-catalyst)

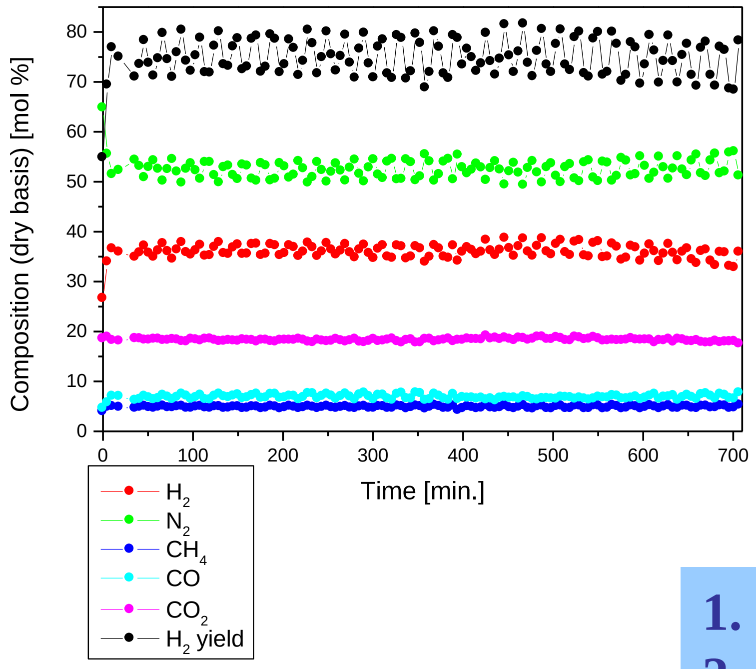

Specific surface area and catalytic activity of $La_{0.6}Ce_{0.4}Fe_{0.68}Ni_{0.2}K_{0.12}O_3$ catalyst **synthesized by different CS methods**

Synthesis Method	BET initial, m²/g	BET, after reaction, m²/g	Conversion, %
VC	21.3	4.4	72.3
SGC	27.9	4.9	68.5
IPC	28.6	5.3	77.8
ISC	48.8	38.3	58.7

1. **Highest conversion was achieved by IPC-catalyst**
2. **Catalytic activity does not directly correlated with catalyst specific surface area**

Polarization Curves for Methanol Oxidation

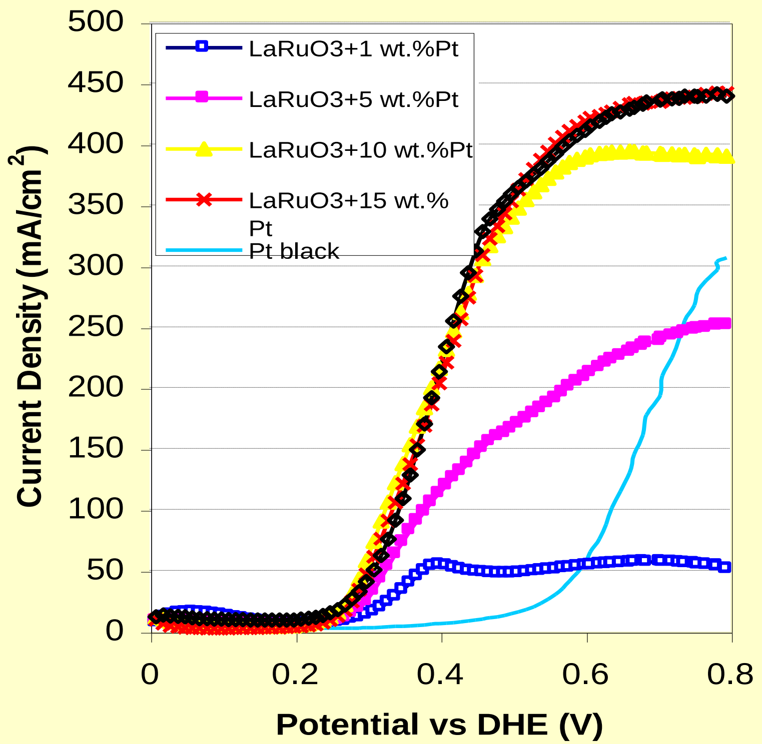

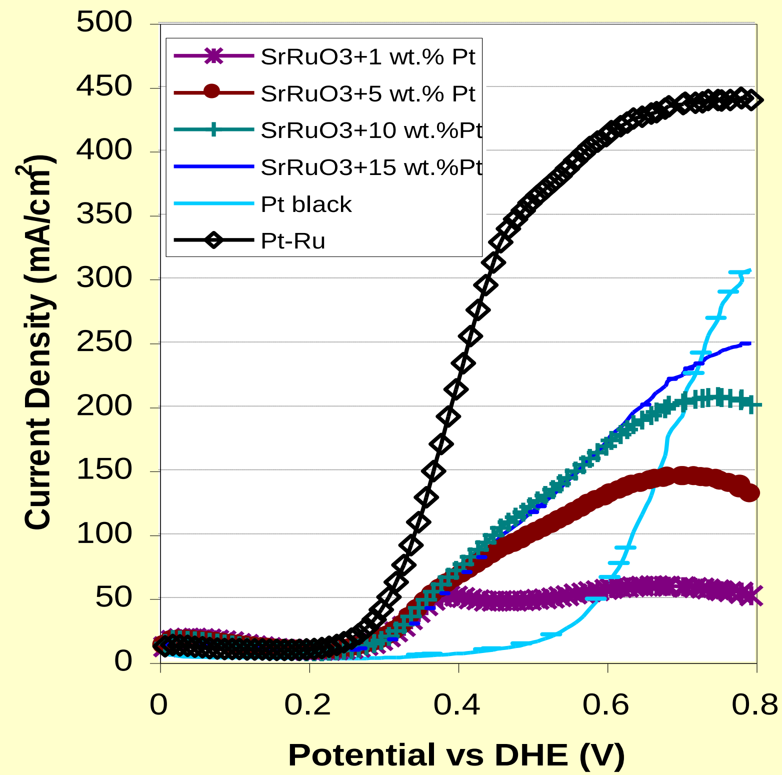

8ml/min, 0.5 M, 20 mV/s and 90 °C

Lan, A. and Mukasyan, A. ECS Trans. 2, (24) 1 (2007).

It works ! Perovskite+Pt > Perovskite or Pt black

LaRuO3+10 wt.% Pt ≈ Pt-Ru ! (with much lower Pt loading)

Potentiostatic Results

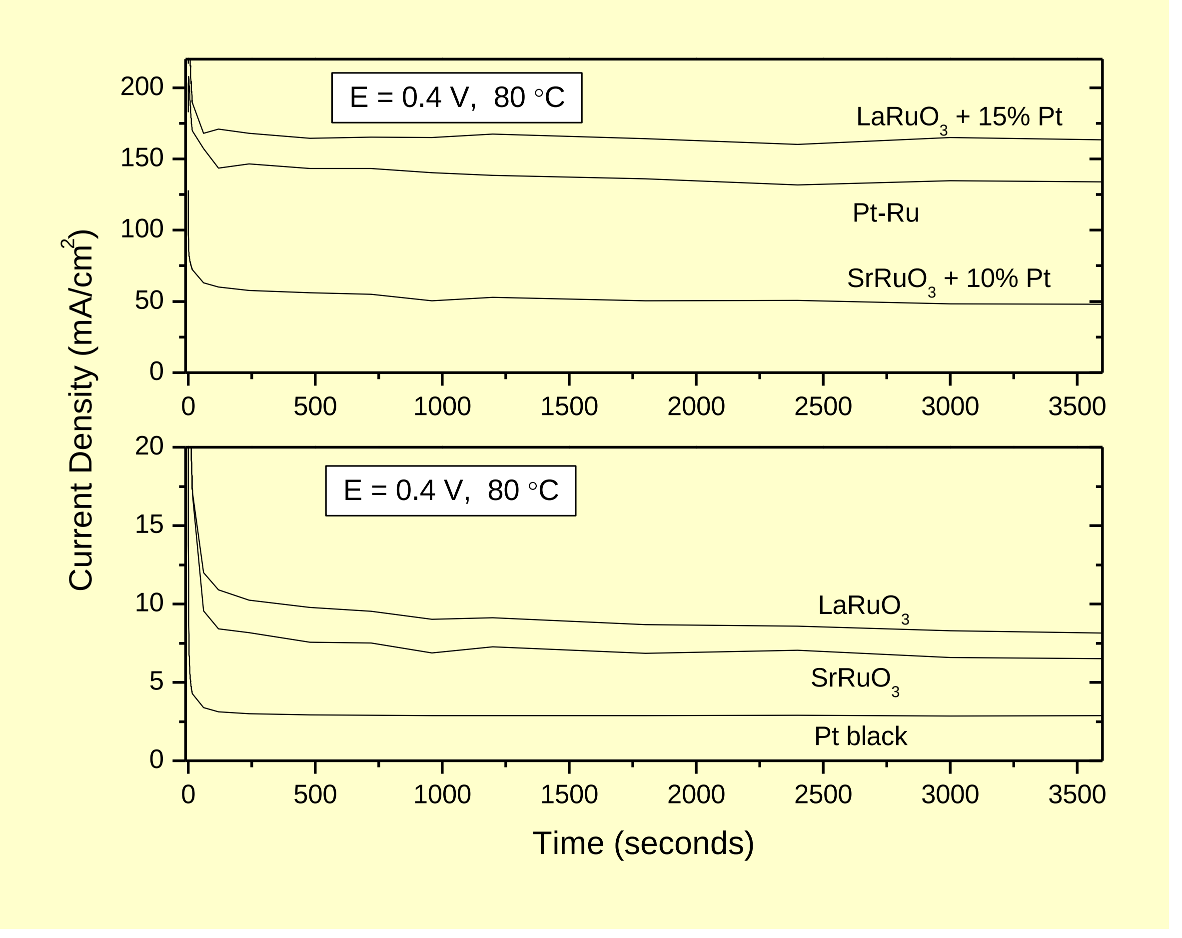

Lan, A. and Mukasyan, A. *J. Phys. Chem,* 26, 9573 – 9582 (2007).

Conclusion

Solid Flame - *phenomenon of rapid reaction propagation in gasless heterogeneous exothermic systems,* ***being extremely interesting from fundamental point*** *of view*, *also allows development of a variety of* ***effective, energy saving technologies*** *for synthesis of advanced materials.*